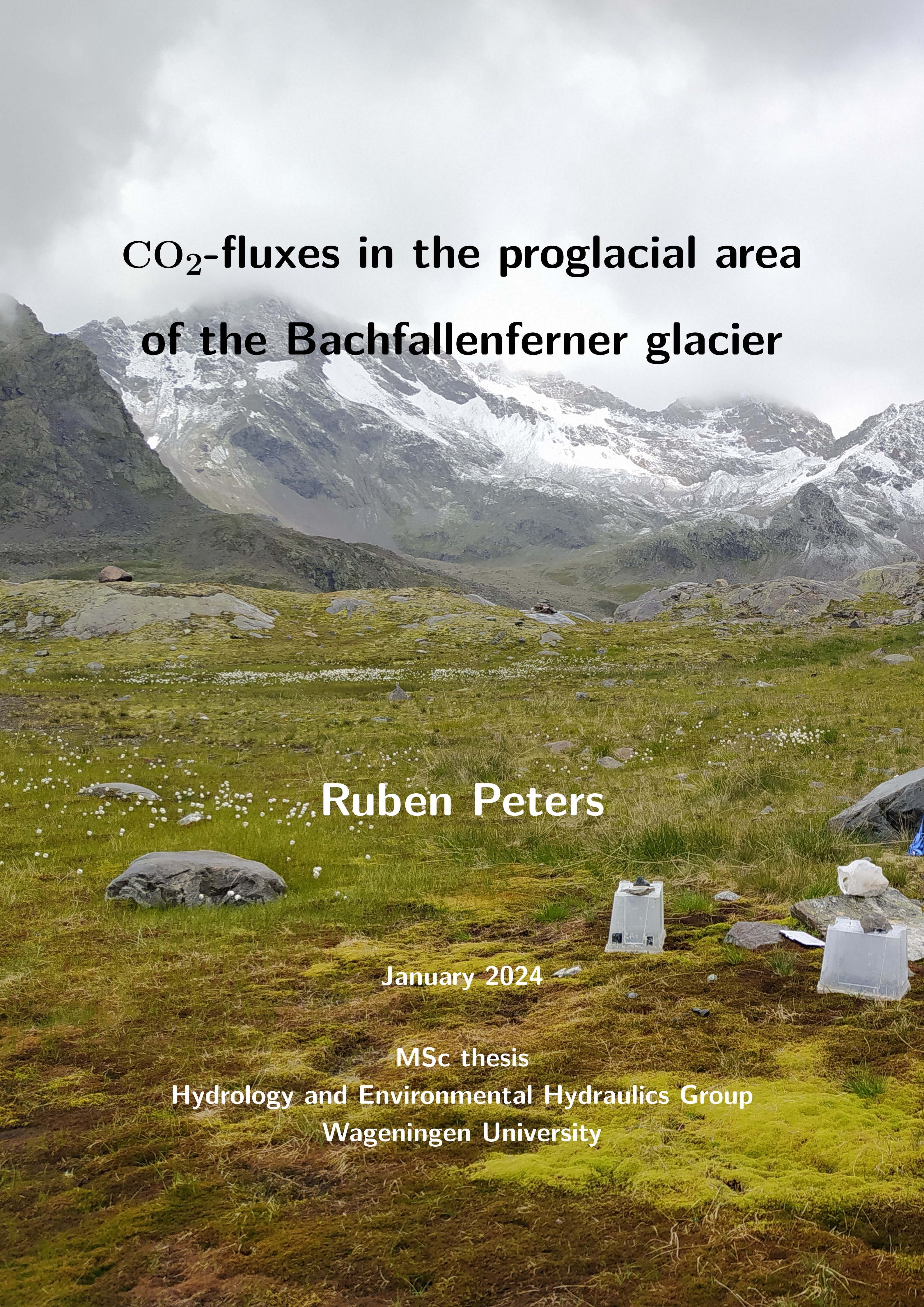

CO_2-fluxes in the proglacial area of the Bachfallenferner glacier

Ruben Peters

January 2024

MSc thesis
Hydrology and Environmental Hydraulics Group
Wageningen University

Abstract

Global warming continuously leads to deglaciation of mountains, enlarging the extent of proglacial area across the Alps. These newly exposed soils could have a significant role in the global carbon budget, however relatively little is known about the processes that affect CO_2-fluxes in these areas. This thesis aims to quantify daytime August CO_2-fluxes of wetlands and soils in the proglacial area of the Bachfallenferner glacier, in order to relate these values to several potentially influential variables. Soil moisture content was identified as a primary variable reducing CO_2-emissions. Reasons for this likely include increased soil development, vegetation growth and reduced respiration rates. The locations with the highest soil moisture content were often local depressions. Soil moisture content and soil organic matter content were found to highly correlate with one another. Grasses were the vegetation type with the highest correlation with the fluxes measured in the area. Mean daytime fluxes remained around 0 for soils up to years 84 of age. Between age 119 and age 174, mean daytime fluxes of -6.92g $CO_2\times$ m$^{-2}\times$ d^{-1} were found. No clear impact of radiation and precipitation conditions could be distinguished. Possible additional variables of influence are pH, (soil) temperature and availability of nutrients. The results emphasize the role of soil moisture in carbon fixation from the atmosphere by proglacial soils. Increased frequency of climate change-induced drought events could pose a risk for reduced carbon storage in proglacial areas.

Contents

1 Introduction

Global warming has worldwide consequences. However, there are few places where the impact is as visible as in glaciated areas. One region in which those areas are found is the Alps. During the mid-19th century, Alpine glaciers began to retreat abruptly. This process has been going on ever since, albeit with some periods of glacier re-advances in the 1890s, 1920s, 1970s and 1980s. After 1981, uniformly negative mass balance years dominate (Zemp et al., 2008). Between 1850 and 1970, the loss of glacial area amounted to around 35 percent of its total. In 2000, this had reached almost 50 percent (Zemp, 2006).

Initial melting from the 1850s onwards was likely due to industrial black carbon deposition in snow and snowmelt, which significantly reduced the albedo of these glaciers (Painter et al., 2013). Later on, the dominant factor became rising temperatures. This will likely remain the case in the near future. Due to the dependency of temperature increase on elevation, the Alpine regions above 2000m are especially vulnerable to climate change. Kotlarski et al. (2012) suggests that at these elevation levels, increase in mean summer near surface temperature at 2 meters height might exceed 5 degrees Celsius between the 1961-1990 and 2070-2099 periods. The warming of these regions has caused a rapid retreat of glaciers, with an average yearly decrease of 39km^2 of glaciated area between 2000 and 2014 (Sommer et al., 2020).

The areas where glaciers have retreated from are known as glacier forefields or proglacial areas. Here, we now find predominantly dry soils and bare rock, but also wetlands, lakes and small water streams from the glacier. The reason for the formation of different types of land cover is that they are influenced by different factors depending on the composition of their materials and position in the landscape. These factors include: slope steepness, slope position (higher/lower and north/south exposure to the sun), parent material, soil age and water availability as well as a number of chemical factors.

Soil development usually starts with the formation of a microbial community. The formation of these communities is highly heterogeneous, but their structure and composition are mainly affected by water content and soil age (Noll and Wellinger, 2008). These initial heterotrophic communities use ancient recalcitrant carbon (Bardgett et al., 2007) and/or black carbon that is either atmospherically deposited or left behind after melting of the glacier (Eckmeier et al., 2013). Depending on the soil development its conditions will become suitable for plant growth. After more than 50 years of exposure, Eckmeier et al. (2013) suggests that the microbial community changes to one supported primarily by carbon derived from modern plant growth, most likely due to recent plant production. This is confirmed by Guelland et al. (2013), which concludes that new plant-fixed carbon becomes the main source for soil respiration after 58-78 years. After further soil development and accumulation of soil organic matter, heterotrophic respiration again increases relative to using plant-fixed carbon.

Carbon accumulation in the young soils of these ecosystems appears to decrease in efficiency with time. This is illustrated by the proglacial area of the Damma glacier in Switzerland, where the ratio between carbon accumulation and soil carbon flux decreased from 11 to 0.4 in soils respectively 7 and 110-128 years of age (Guelland et al., 2013; Smittenberg et al., 2012). Multiple other studies confirm the trend of a rapid rate of carbon accumulation in young soils (Mavris et al., 2010) and a decrease in this rate when looking at older ages in a chronosequence (Schlesinger, 1990).

One of the things that all of the above studies have in common, is that they conduct an analysis on (proglacial) soils, while wetlands are not investigated. Wetlands in general are known to have the potential to be either a sink or a source (especially when disturbed) of carbon (Roulet, 2000); (Mitsch et al., 2013). The carbon cycle in wetlands is complex. Some major environmental factors determining the net influence regarding the carbon budget include water saturation and (soil) temperature. Saturated water conditions reduce oxygen availability, limiting both aerobic respiration (Han et al., 2018) and decomposition (Moomaw et al., 2018). Low temperatures, often present in proglacial areas, are associated with lower rates of decomposition as well. On the other hand, higher temperatures could increase primary production (as long as it does not lead to drought) through more photosynthesis (Salimi et al., 2021). Nevertheless, increase of deposition rate would likely be larger than increase in primary production, suggesting that lower temperatures could be more favourable conditions for carbon storage. Furthermore, soil acidification could reduce CO_2-emissions by microbial communities.

CO_2-fluxes in proglacial areas follow both a diurnal and seasonal cycle. Uptake of CO_2 mainly takes place through during daytime, while during nighttime respiration causes a net efflux of CO_2. During summertime, the carbon cycle is most active. During the winter season, in snow-covered conditions, there is no diurnal cycle and usually net emissions are observed (Koch et al., 2008).

This research elaborates on the work done by Janssen (2023). This study has conducted a similar research in the Martelltal in the Italian Alps, quantifying CO_2-fluxes in the proglacial area of the Cevedale glacier. It found that uptake of CO_2 changes with soil age, and suggests that wetlands are major carbon storage hotspots. However, the amount of wetland measurement locations in the research was relatively low (28 measurements, 4 wetlands). To be able to draw more powerful conclusions, a field campaign with more wetland measurements is needed.

Compared to Janssen (2023), the amount of wetland locations selected in this study is larger. A total of 24 wetland locations were measured (with 63 successful individual measurements conducted). 15 of those are coupled with a soil point that is located near, as much as possible in the same conditions, except for soil moisture level. Additionally, in this research, soil moisture conditions are not only divided in categories (e.g. soil, wetland), but soil moisture is quantified as well, using the soil moisture mass-percentage. This way, a more specific and quantifiable relation between soil moisture and CO_2-fluxes can be investigated.

Furthermore, the relations between flux data and carbon stock data were investigated. The method for researching relations between flux and soil age/vegetation are largely similar, but the total amount of measurements was higher (212 compared to 129). The extra data could either strengthen or contradict results from Janssen (2023). The data of this research were gathered at the Bachfallenferner glacier. This is the first time that this glacier is included in a research of this kind. No English publications have been produced on the Bachfallenferner glacier.

The objective of this research is to quantify carbon flux values of wetlands and soils in the proglacial area of the Bachfallenferner glacier, in order to relate these values to soil moisture, vegetation, soil age and carbon stock, as well as further data gathered. The main focus is on the influence that soil moisture conditions have on the CO_2-flux coefficient (in this study defined as change in ppm CO_2 per 30 seconds), and potential differences found between wetlands and their dry soil counterparts.

A number of questions has been formulated in order to reach the objective. All of the questions relate to the Bachfallenferner proglacial area. The main research question is:

To what extent are carbon flux measurements of predictive value for determining carbon stock in wetlands and soils in the area?

Sub questions:

1. Is soil moisture the key factor in determining the CO_2 flux of specific locations in the proglacial area?

2. Does the presence of vegetation cover significantly influence CO_2 flux in soils with similar age and moisture conditions, and if so, which species play the largest role?

3. Does soil age play a significant role in determining the CO_2 flux of wetlands and soils in the area?

2 Methodology and data

2.1 Field site

The field site chosen for this research is the Bachfallenferner proglacial area, which is located in the Stubai Alps in Austria, adjacent to the Ötztal (Figure 1). It is part of the Austroalpine basement region (Alagna et al., 2010). The glacier itself is positioned in the southeast of the research area (Figure 2), which is characterised by two plateaus separated by a steeper section in the middle. The first plateau is located at the glacier terminus, here the youngest soils are positioned.

Figure 1: Region of Austria in which the research area is located, depicted inside the black square bottom left (FreeWorldMaps, 2023).

This plateau has an elevation of roughly 2650 to 2700m, and this is where the largest lake (centre of Figure 2) can be found. Directly west of the glacier a thin strip of land is accessible by foot. With an elevation of up to 2900m is the highest area of the field site. The second plateau is situated in the northwest of the area, at an elevation of around 2500m and hosts a number of smaller lakes. The steeper section between the plateaus is unsuitable for conducting measurements, except for locations close to the footpath. A stream runs westwards from the large lake through the steep section and the second plateau (from this point on referred to as "lower" plateau).

This area was chosen due to a combination of factors. First of all glacial retreat is well documented here (see glacier extents in Figure 2). Furthermore, the area is easily accessible and home to a number of wetlands and lakes from different ages that could be recognized from satellite imagery before the actual field campaign. The field campaign was conducted in an elevation range of roughly 2400 to 2900 meter AMSL. The area in which the samples were taken has a size of 0.86 km^2.

2.2 Sampling design

The sampling design mainly concerns two different components: determining the locations where the sampling should be done, and determining what data should be gathered at these locations. The latter can be found more

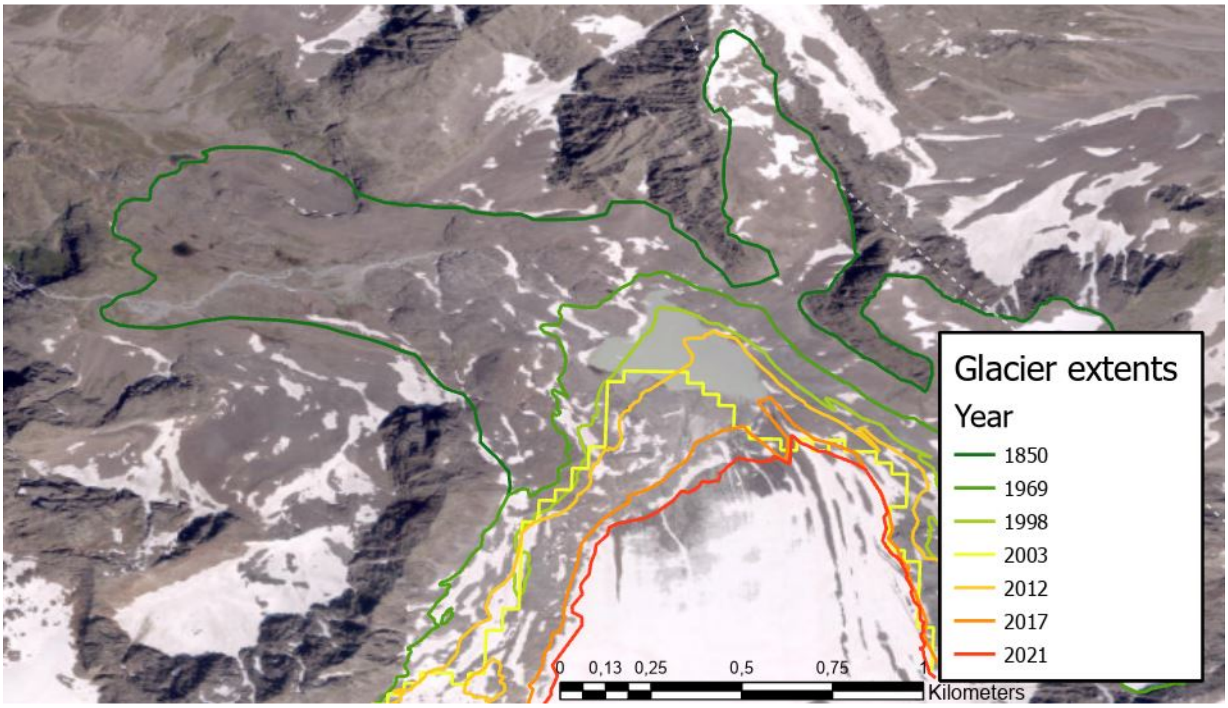

Figure 2: The Bachfallenferner glacier field site, with the glacial extents between the years 1850 and 2021 depicted. Adapted from ArcGIS Pro (2023).

extensively in Appendix A.

The sampling locations were decided on through a Latin hypercube sampling method (Minasny and McBratney, 2006). This method, which is run through an R-script, generates a near-random sample that takes into account the distribution of different parameters. The parameters used in this case are slope, soil moisture and soil age. The slope is based on the 10 meter DEM-raster from data.gv (2023), via ArcGIS. With an extended version of this ArcGIS model, the topographic wetness index (TWI) (Sørensen et al., 2006), a steady state wetness index, was determined. This is used as a proxy for the soil moisture content. Lastly, the soil ages in the area were determined. This was also done in ArcGIS, through a series of six different models, partly distributed by Professor Arnaud Temme of Kansas State University. The soil age raster is, the DEM aside, based on GLIMS glacier polygons, which includes data of the glacier extent in 1850, 1969, 1998, 2003 and 2012 (NSIDC, 2023). The glacier extents of 2017 and 2021 were added manually to this set based on the satellite imagery on Google Earth Pro (Pro, 2023), making a total of seven glacier extents (Figure 2). By interpolation between these extents a complete soil age raster for the area was made. In order to get better results, a support line was added through the middle of the proglacial area. This line is based on a cost path with as inputs the filled DEM as cost distance raster and Flow Direction as cost backlink raster.

As mentioned, the above parameters were inputs for the Latin hypercube. On top of that, some locations in the research area were excluded from the Latin hypercube sampling. These are the locations that were considered to be too steep and floodplains, which were both assessed visually through Google Earth Pro imagery. The former locations were excluded for safety reasons, the latter because floodplains are not representative locations for the soil age. This is due to the fact that on the floodplains significantly more sedimentation processes take place, causing the fine earth materials to be of a different age compared to the time since exposure of the location itself. In other locations this was deemed to be less of a problem. Even though erosion takes place throughout the research area, this concerns mainly larger boulders and rocks, which have a negligible effect on soil formation.

In the first run of the Latin hypercube sampling method, 40 locations were selected. In the second run, 32 further locations were selected. Two runs were done to cover for a situation in which it would not be possible to visit all of the sampling locations in the available time for whatever reason. By first doing 40 priority points, it is certain that at least all relevant variation inside the research area is covered.

An important factor in this research is the focus on wetlands. To make sure enough data would be gathered for this type of land cover, fifteen wetlands were manually selected based on Google Earth Pro imagery. To be able to directly compare results from wetlands with non-wetlands, fifteen dry soil locations adjacent to the wetlands were selected. These were expected to have similar characteristics as the wetlands, except for soil moisture conditions. Since the wetlands needed to be verified in the field, ten more wetlands were identified as alternative points, or additional points in the case that the field campaign progress would be more rapid than expected.

2.3 Field campaign

The field campaign consists of location descriptions, soil sampling and CO_2-flux measurements. The full sheet used in the field can be found in Appendix A.

The first action on any location was conducting a location description. The location description consists of the following aspects: Location ID, type of location (soil, wetland, lake), date and time of observation and group number were written down. Four pictures were taken: one of the 100 m^2 of the location, one 1 m^2 surface location, one picture of the chambers, and one picture of the same location with the chambers removed. For the weather, it was noted if it was sunny, partly cloudy or cloudy. Partly cloudy is defined as a situation in which the surrounding visible ground is partly covered by a cloud shadow and partly in the sun. In sunny conditions the complete surrounding visible ground is in the sun, in cloudy conditions it is completely overcast. Furthermore, it was noted whether there was precipitation during the measurement, if there has been precipitation in the past 1 or 12 hours, or if it was dry.

GPS coordinates, slope, aspect, plan/profile curvature, signs of erosion/deposition, current or past connection to a river system were also assessed. Additionally, it was noted whether the location was a wetland and if it was a local depression in the landscape. Lastly, surface cover was assessed over the 1 m^2 surface in percentages. The categories for this are bare hardrock, stone, fine earth, grass, plant, moss and surface water and should add up to 100

At each possible location, soil samples were taken. This was for later analysis on soil moisture, soil organic matter content and pH in the lab. If a soil consisted of multiple horizons, each horizon was sampled. In order to have enough material all of the analyses, each sample should contain at least 100 grams of fine earth. First, the soil saturation at 10 cm depth was assessed with the categories saturated, moist and dry. Then for every horizon, the following things were written down: horizon ID, horizon code, horizon start depth and end depth, texture, total rock fragments, rock fragment size, rock fragment shape, soil structure grade, soil structure type, root abundance, root size and whether there was any biological activity visible other than roots.

For the CO_2-flux measurements, a total of six K33-ELG sensors from SenseAir (2023), (Figure 4) were used. In addition to measuring the CO_2-concentrations (in ppm), these sensors have the ability to measure temperature (in degrees Celsius) and relative humidity (in %). The values of these variables are determined every 30 seconds, and stored into the sensor's memory. The sensors were calibrated every morning between 7:00 and 8:00. This was done outside every time, except for 7 August. The calibration value used for the CO_2-concentration was a standard estimate of 450 ppm. The exact value of this calibration is not important, because it is the change in concentration that is relevant for the research, not the concentration itself. However, to prevent any potential difficulties during the data analysis, it is was deemed better to choose a realistic value and prevent the device from registering negative concentrations. The temperature calibration was based on a personal estimation, and therefore not suitable for interdaily analyses. The relative humidity was not calibrated.

In order to achieve a number for the flux, a closed chamber approach was used. The method of usage is based on Bastviken (2015), with an improved connection mechanism. The closed chamber is a transparent plastic box (Figure 3), in which two smaller plastic boxes are assembled. One of these is for the fragile sensor, to protect it from its environment, the other one stores the battery. The area of the chamber over which the flux is measured is 0.28 m x 0.39 m = 0.1092 m^2.

Due to the rough terrain that is found in the area of research, it is important to have a flexible way to seal the chambers to the ground. To solve this potential problem, reusable clay was used. It was attached to the edges of the chamber, mostly around 3 centimeters high, and then pushed into the ground. Subsequently, the remaining gaps between the clay and the ground were filled by working the clay or adding more. Additionally, stones or finer naturally occurring materials in the area were used. In lakes or wetlands the use of clay was often not required, because in these environments the chamber is usually sealed off well by either a small layer of water or a very flat surface in which the chamber can be pushed slightly. The last measure to make sure the box is stably sealed was addition of a stone on top of the chamber.

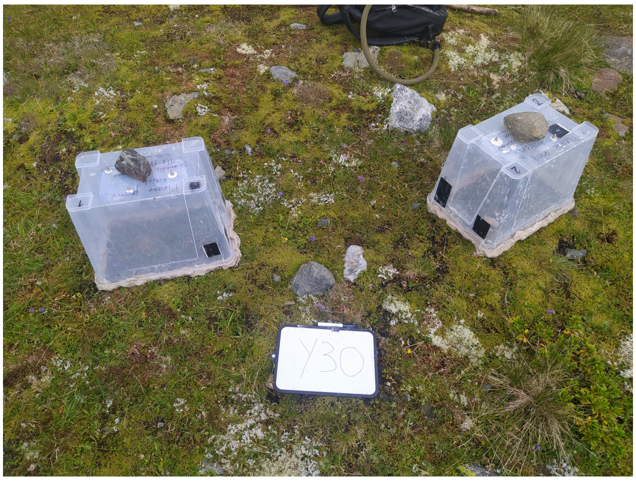

Figure 3: Field setup of location Y30.

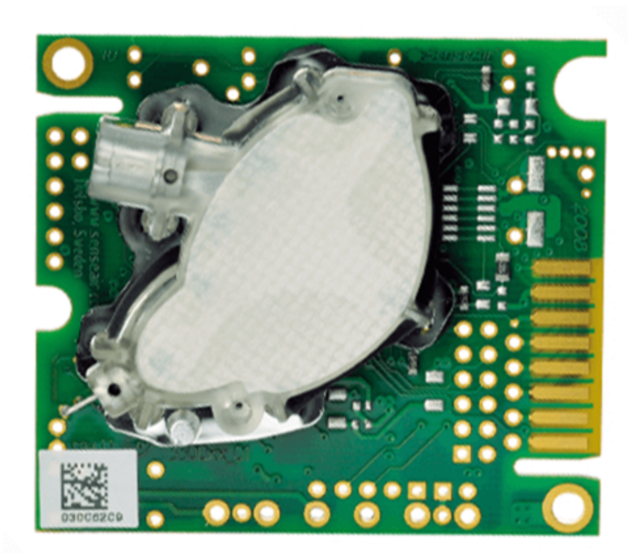

Figure 4: K33-ELG Sensor (retrieved from SenseAir (2023)).

In the field, the process was as follows. First, measurement location ID, chamber ID's and date were written down. Then the clay was attached to two chambers at the same time, and the chambers were attached to the ground. After checking whether the sealing is airtight, the starting time was noted, accurate to the second. The checking process was required to be both accurate and quick, since the accumulation or reduction of CO_2 starts as soon as a chamber touches the ground. It is desirable to keep this time below one minute. After noting the starting time of the measurement, the quality of the connection to the ground (good/medium/bad) was noted, as well as whether flow of air from underneath the ground could be expected. This could be the case when a surface consists of mainly rocks and other large materials, which leaves gaps in the ground where airflow could occur. Lastly, an assessment was made of whether the two chambers are placed on a similar kind of surface, and whether that surface was representative for the 10x10 meter surroundings. In some cases it was more desirable to use a non-representative surface. Examples of this are measuring a small wetland with dry soil surroundings, or a location with an uneven terrain where only a small flat surface was available for a decent connection of the chamber to the ground. The flux measurements were done four times per location. This consisted of two spatial replicates, and two temporal replicates. Each individual measurement took 10 minutes.

2.4 Lab work

Soil samples (at least 100g fine earth material per location) were analysed in the lab. The three types of results gathered from the lab work were soil moisture content, soil organic matter content and soil pH. All of the weights were measured in (g), the soil moisture and soil organic matter content in percentage of total mass. The soil moisture content was determined in the following way:

1. Weighing tray
2. Weighing tray with wet soil
3. Drying soil in the oven at 105°C for 24 hours.
4. Weighing tray with dry soil
5. Calculation:

$$Moisture\% = \frac{M_{\text{tray+wet soil}} - M_{\text{tray+dry soil}}}{M_{\text{tray+wet soil}} - M_{\text{tray}}} \times 100 \quad (1)$$

After this process, all samples were sieved to remove any stones and gravels (> 2mm). For the soil carbon content the following method was used:

1. Weighing crucible
2. Weighing crucible with dry soil
3. Ashing soil in the oven at 550°C for 4 hours
4. Weighing tray with ashed soil
5. Calculation:

$$OM\% = \frac{M_{\text{crucible+dry soil}} - M_{\text{crucible+ashed soil}}}{M_{\text{crucible+dry soil}} - M_{\text{crucible}}} \times 100 \quad (2)$$

The pH was determined after combining 5 grams of fine earth material with 45 ml of demi water.

2.5 Data analysis

From the raw data on CO_2-concentrations, fluxes were determined based on an adapted version of an R-script constructed by Janssen (2023). This script makes a best tangent estimation for each of the concentration time-series. This tangent should contain at least five data points (measured over 4 × 30 seconds = 120 seconds), and start no earlier than the second data point. When no tangent is achieved, the process is repeated from the third data point, then the fourth, until at least one tangent is made. A minimum of five data points was considered enough, and even preferable over longer time series, because interest goes out to the initial increase or decrease in CO_2 inside the chamber. After a longer time, CO_2-saturation might occur in the chamber. The first data point was always skipped in order to avoid any error that might have occurred during the installation of the chamber.

At each location, four flux measurements were conducted, two spatial and two temporal replicates. In order to get a representative flux for the location, these fluxes were averaged. This is the value that was used for the analyses. In order to include only good quality measurements, a cutoff of ≥ 0.7 was chosen for R^2. This is consistent with Janssen (2023), and allows for the inclusion of measurements done on rocky terrain, which are usually subject to more noise. Because of this, not every location has all four measurements included in the averaging process. For 22 locations, all four measurements were used. For 20 locations, three were used. For 25 locations, two were used. For 14 locations, only one measurement was used. In some cased this led to the complete exclusion of a location.

The total dataset suitable for conducting analyses consists of 80 locations. This is a combined dataset that includes the following 25 columns: LocationID, date, time, latitude, longitude, mean flux, year of exposure, soil moisture, steepness, aspect, cloudiness, precipitation, all of the surface cover types, total organic matter, topographic wetness index, elevation and soil age.

For the statistical analyses, the first step was always to determine whether or not the data was normally distributed with the Shapiro-Wilk test. This was the case for every variable in every analysis, because even if a variable was used in multiple analyses, results could differ because of the amount of data points used. For instance, soil moisture data was available for 77 out of 80 points. Surface cover data was available for 74 out of 80 points. Both of these variables were used for comparison with the flux data. Since it is desirable to use all available data, in the former case 77 flux points were used, whereas in the latter only 74 flux points were used. This obviously causes different results in the Shapiro-Wilk normality tests.

For analyses on correlation, either Pearson's r or Spearman's ρ was used. The former if both variables were normally distributed, the latter if one or more variables were not normally distributed.

To test whether there were significant difference between two groups, t-tests were done for normally distributed data, and Wilcoxon rank sum tests for non-normal data. For other analyses with more than two variables, ANOVA was used. One multiple linear regression was done in an effort to improve the proportion of the variance of the flux coefficient that is explained in a single model. Lastly, a principal component analysis (PCA) was conducted to present an overview of which numerical variables are most strongly linked to one another. Average values of pH (used in Table 1) were retrieved by first converting to linear scale ($10^{-\mathrm{pH}}$) and averaging over those number before converting back to logarithmic scale, in line with Eralp and Tomson (1978).

In order to correct for weather differences, a "radiation filter" was constructed. This filter makes use of an addition factor based on time of day, cloud cover and vegetation. Time of day is known for every measurement, as well as whether it was sunny, partly cloudy or cloudy. The total vegetation cover is known, with subdivisions into grass, plants and moss. Since radiation and photosynthesis are tied (Sinclair and Horie, 1989), it is likely that during sunny circumstances a more negative flux is registered than when it is partly cloudy or completely overcast. This is where the addition factor comes in: it compensates for the negative influence that radiation in sunny conditions has on the flux, by adding a number to it. This number (referred to as F_{add} depends on the time of day, cloud conditions (Figure 5) and vegetation cover. The sinusoidal curve is defined as follows:

$$F_{\mathrm{add}} = Max_{\mathrm{add}} \times sin(2 \times \frac{t + 1.375}{29.5} - \frac{pi}{2}) \times \frac{Veg_{\mathrm{tot}} - Moss}{100} \quad (3)$$

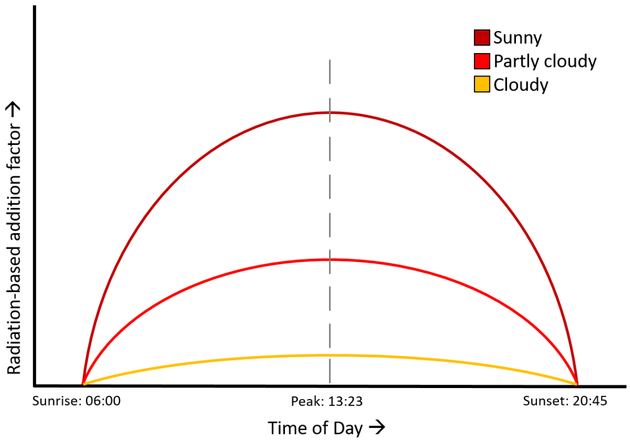

Figure 5: A simplified schematic of the radiation filter. Max_{add} values are reached during peak-time, when the sun is highest above the horizon. This figure does not take into account the percentage of vegetation cover (excluding moss), which is used in the equation.

This curve crosses the x-axis at exactly 06:00 and 20:45 (Maplogs, 2023), roughly the times of sunrise and sunset in the area during the field campaign. The maximum addition for sunny, partly cloudy and cloudy weather is reached when the sun is at its highest point; this is around 13:23 during the week of the field campaign.

Since this method is based on a link between photosynthesis and radiation, vegetation should be taken into account. Moss is excluded from the equation, because of its low photosynthetic activity (Aro and Gerbaud, 1984), and lack of correlation with the CO_2-flux values. For a location that is 100 percent covered with vegetation (excluding moss), the full addition factor is added. For a 50 percent vegetation coverage, the addition factor is divided by 2, etc.

The maximum addition for the three cloud condition types is determined using a for-loop. This loop constructs a linear regression model for the radiation filtered flux with another variable of choice. Any combination of the three maximum additions is run from 0 to 10 with step size 0.1. The regression model with the maximum R^2 is chosen to be most suitable. With the vegetation coverage and the maximum addition per cloud condition type known, the addition factor for every flux measurement can be calculated.

Daily CO_2-fluxes used for comparison in the discussion were calculated an adapted version of equation 1 by Janssen (2023):

$$Flux(\mathrm{g} \times \mathrm{d}^{-1} \times \mathrm{m}^{-2}) = \frac{Flux(\mathrm{ppm/30s}) \times 6.64 \times 10^{-6}}{30} \times \frac{44.01 \times 86400}{0.1092} \quad (4)$$

In this equation, the flux is divided by 30 to get to ppm/s, 6.64×10^{-6} is to convert from ppm to mol particles inside the chamber, 44.01 g/mol is the molar mass of CO_2, 86400 is to go from second to day, and 0.1092 m^2 is the surface area of the chamber (0.28m $\times$ 0.39m). For calculations using C instead of CO_2, the molar mass of 12.01 g/mol is used instead.

3 Results

The results are made of various aspects, which combine to answer all of the research questions. Exact p-values for the Shapiro-Wilk normality tests can be found in Appendix B. For all of the results the full dataset of 80 locations is used with all available data, unless stated otherwise. The significance threshold of any p-value is decided to be the generally accepted threshold of $p<0.05$.

3.1 Soil moisture

Manually selected wetlands were coupled with adjacent dry soil locations with characteristics as similar as possible. A total of 14 of these pairs could be made where every location has at least one measurement with an R^2 over 0.7. Given the normal distribution of fluxes in both the wetlands and soils, a paired t-test was deemed the appropriate statistical method. This test resulted in a p-value of 0.27, indicating there is no significant difference between both variables. However, in this sample the measured wetland flux coefficients are more consistently negative (12 out of 14 locations, Figure 6), compared to the soil flux coefficients (9 out of 14 locations).

For the regression of soil moisture against CO_2-fluxes of 77 top-soils, a discernible pattern emerges. As soil moisture increases, the flux shows a negative trend, with an R^2 of 0.21 (Figure 7). The flux follows a normal distribution, the soil moisture data does not. Therefore a Spearman's rank correlation coefficient is determined, with a result of $\rho = -0.41$ ($p = 2.4 \times 10^{-}4$). This indicates a moderate negative correlation.

To conduct an ANOVA on the soil moisture data, it is subdivided into three classes (low: mass-% < 33, middle: mass-% ≥ 33 & < 67, high: mass-% $\geq$). The low ($n = 51$), middle ($n = 21$) and high ($n = 8$) class are all normally distributed (Figure 7). Highly significant differences between the CO_2-fluxes of the different classes are observed ($p = 2.64 \times 10^{-5}$). This implies that soil moisture is a highly influential variable concerning CO_2-fluxes.

Because correlation does not equal causation, it is relevant to check whether the strong correlation found is not merely a result of soil aging influencing both soil moisture and fluxes simultaneously but separately. This could mean that soil development increases soil moisture retention capacity, while fluxes simultaneously decrease because of other processes. Therefore, another linear re-

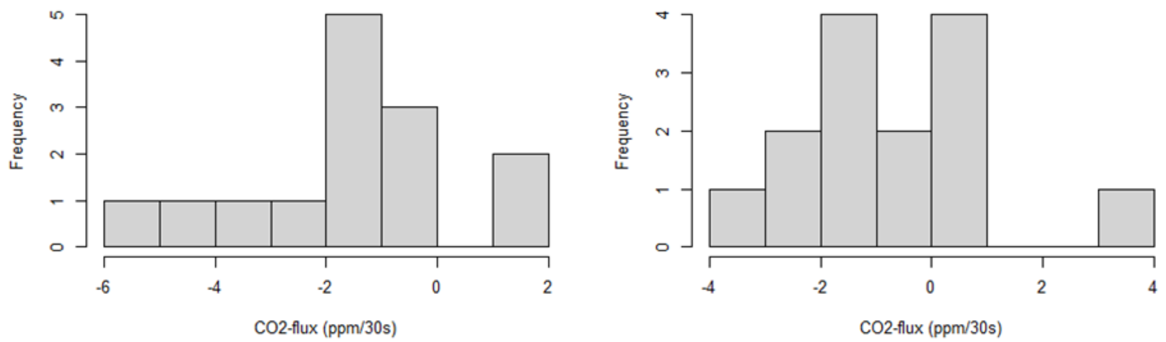

Figure 6: Histograms of the flux coefficients on wetlands and their coupled soil locations.

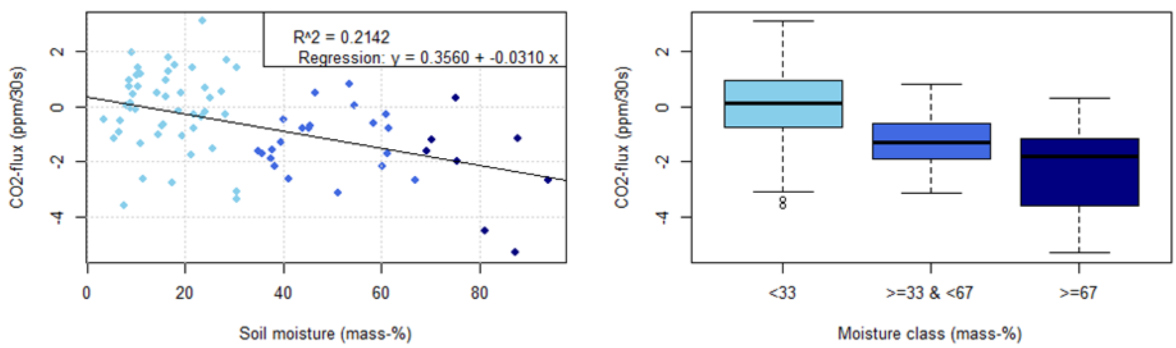

Figure 7: Left: Linear regression of the mass-percentage of soil moisture against CO_2-fluxes. Right: Boxplots of three different soil moisture classes, based on mass-percentages. Low ($n = 51$): $< 33\%$, Middle ($n = 21$): $\geq 33\%$ & $< 67\%$, High ($n = 8$): $\geq 67\%$.

gression was conducted with only soils older than 119 years. These soils (n = 32) are all located beneath the steep section that divides the two plateaus in the field site (more on this in the subsection "Soil age"). In this case a stronger correlation is found than before: $R^2 = 0.27$ (Figure 8). Both groups of data are normally distributed, and the Pearson correlation coefficient yielded $r = -0.52$ ($p = 0.004$), indicating a moderate, albeit stronger than for the full dataset, negative correlation. An additional remark is that to the contrary of the full dataset, almost exclusively negative fluxes are found.

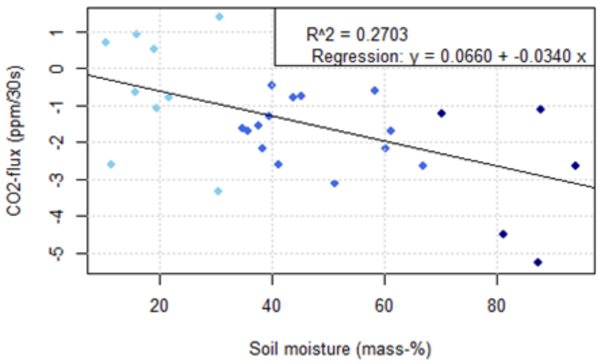

Figure 8: Linear regression of soil moisture mass-percentages against CO_2-fluxes, with only soils aged > 119 years included. The colours indicate the same soil moisture classes as in Figure 7.

3.2 Vegetation

Figure 11 reveals a negative correlation between the total vegetation fraction and the CO_2-flux. More vegetation, in general, is accompanied by a larger negative flux. Especially soils with a predominantly grassy surface cover influence this trend. Moss coverage does not appear to influence the value of the fluxes considerably, whereas plants do not have a sufficient amount of data in the higher percentages to extract any valuable information from it. The CO_2-flux data is normally distributed, but all of the surface cover variables are not. The Spearman's rank coefficients are as follows: -0.36 for total vegetation, -0.12 for moss, -0.28 for grass and 0.26 for plants.

To determine whether the amount of vegetation cover has a significant influence on the flux, a two-sided t-test was conducted. The dataset was split into nearly equal groups of 33 and 32 data points, which both exhibit a normal distribution. The first category is comprised of locations with no less than 50 percent vegetation cover (moss, grass and plants combined). The second group consists of locations with less than 30 percent vegetation cover. The t-test yielded a p-value of 8.8×10^{-4}, suggesting that vegetation cover does significantly influence the value of the flux.

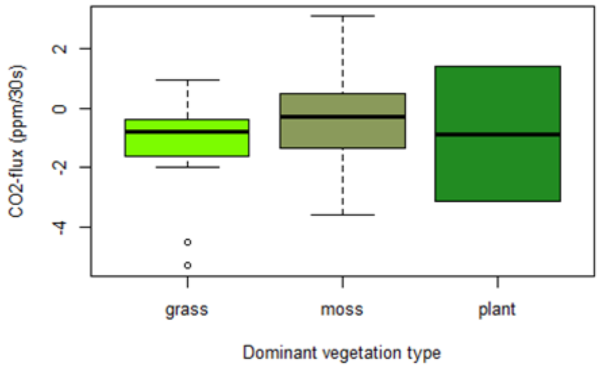

Figure 9: Boxplots of dominant vegetation types. For grass (n = 15), moss (n = 57) and plants (n = 2).

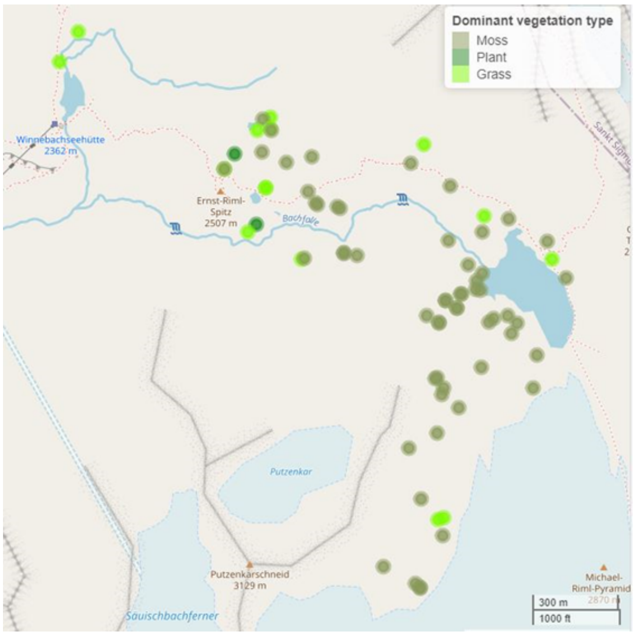

Figure 10: Spatial distribution of dominant moss, grass and plant cover locations.

Furthermore, an ANOVA was conducted to assess potential differences in fluxes among locations characterized by a dominance of moss, grass and plants respectively (Figure 9). Dominant vegetation cover is defined here as the vegetation type with highest surface cover percentage on every location. The test shows that there is no significant difference in flux between the different types of vegetation cover ($p = 0.20$). However, it is noteworthy that the category with dominant plant vegetation cover comprises only two data points, rendering the dataset insufficient for meaningful analysis. Conversely, grass and moss do have more data (15 and 57 points), but no significant differences in CO_2-fluxes were found.

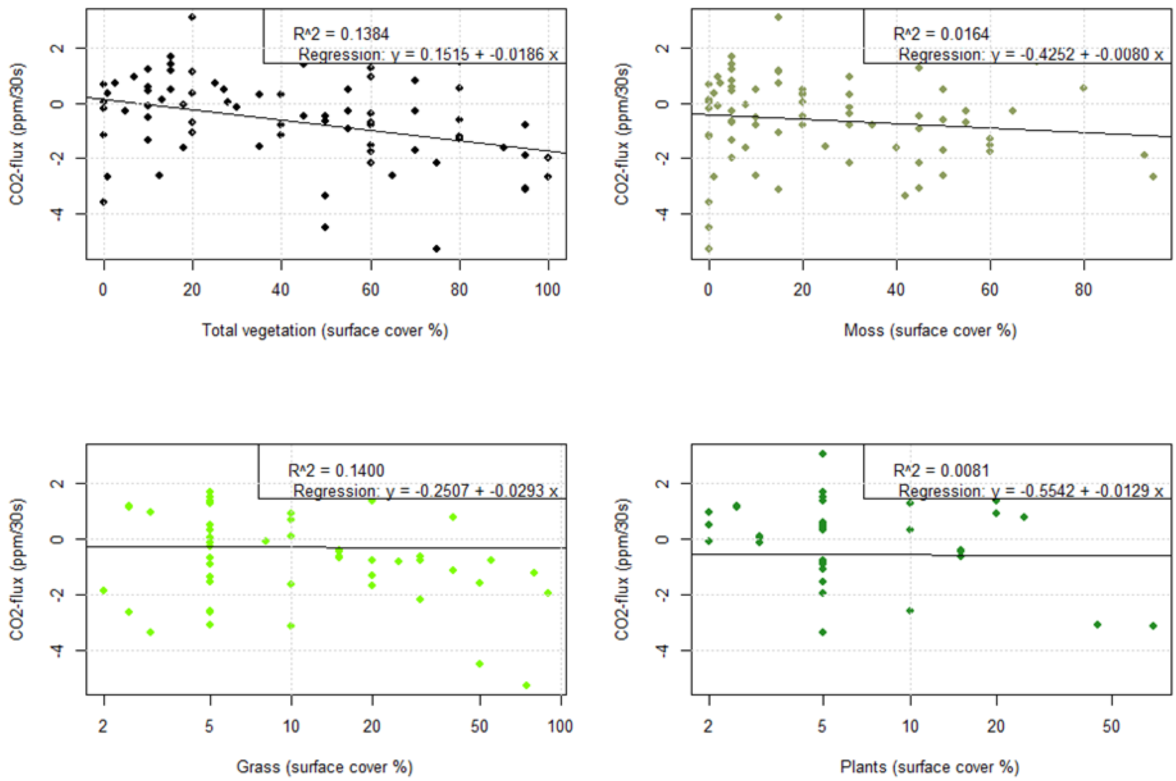

Figure 11: Regressions of total vegetation (top left) and its components moss (top right), grass (bottom left) and plants (bottom right) against CO_2-fluxes. For grass and plants a log-scale is used, since the data of both variables is heavily skewed towards the lower percentages.

Additionally, Figure 10 shows that moss is mainly dominating at higher altitude in younger soils, but also the dominant vegetation type in many soils at lower elevation. Grass-dominated locations are mostly found lower in the landscape, but present throughout the whole research area. The two plant-dominated locations are both found relatively low in the landscape.

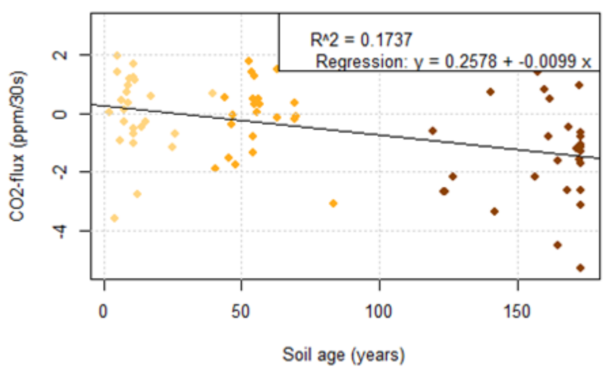

Figure 12: Regression of soil age against CO_2-fluxes.

3.3 Soil age

Soil age could be interpreted as being a passive variable, along which the development of soils takes place, and thereby the evolution of a combination of variables that actively influences the flux coefficient.

Soil ages and CO_2-fluxes are negatively correlated (Figure 12), with an associated R^2 of 0.17. The Shapiro-Wilk test indicates that the fluxes are normally distributed whereas the soil ages are not. Therefore, a Spearman's rank correlation coefficient is computed, yielding -0.41 ($p = 2.4 \times 10^{-4}$). This is again a moderate negative correlation.

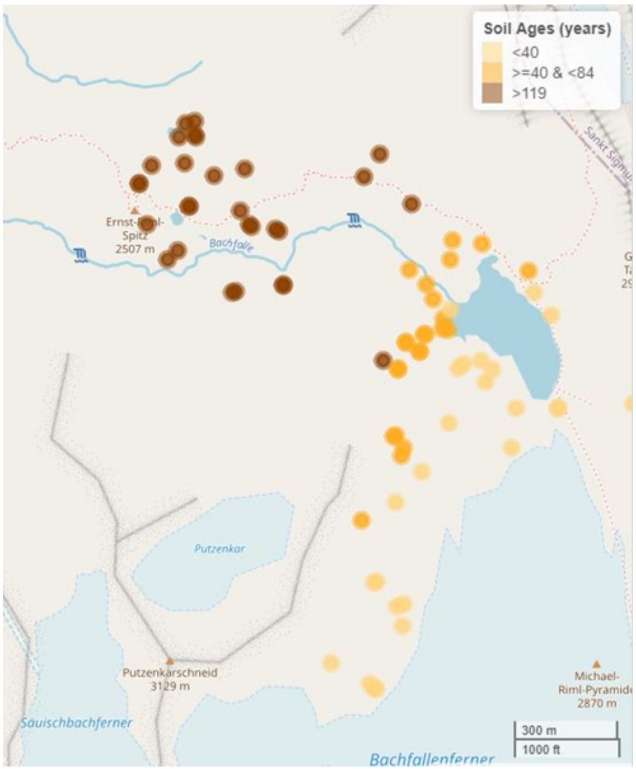

Figure 13: Spatial distribution of soil ages in the research area.

Due to a large step in the terrain, no data could be gathered for soils that got exposed between 1904 and 1939 (thus: soils aged 84 to 119 years). This step is visible in the map in Figure 13, between the clusters of dark-brown and orange locations. The three dark-brown measurements between these clusters were taken along the only accessible path up. Because of this, there are two groups of data widely separated in time . These groups have a normal distribution in terms of CO_2-fluxes. The one-sided t-test for this division of data yielded highly significant results: a p-value of 4.9×10^{-5}.

It has now been established that soil age, soil moisture and total vegetation are all negatively correlated with the CO_2-flux. A combination of all these variables is visible in Figure 14. In this figure, the moss fraction is excluded from the total vegetation cover, because of its relatively small contribution to photosynthesis. What becomes clear from this figure is that the development total vegetation (excluding moss) over time is not enough to explain the change in fluxes over time. Younger soils (<84 years) often have a small fraction of vegetation cover, and have fluxes around 0. When focusing on the older soils (>119 years) with similarly scarce vegetation cover (bottom right of the figure), it becomes clear that these soils have almost exclusively negative fluxes, even under con-

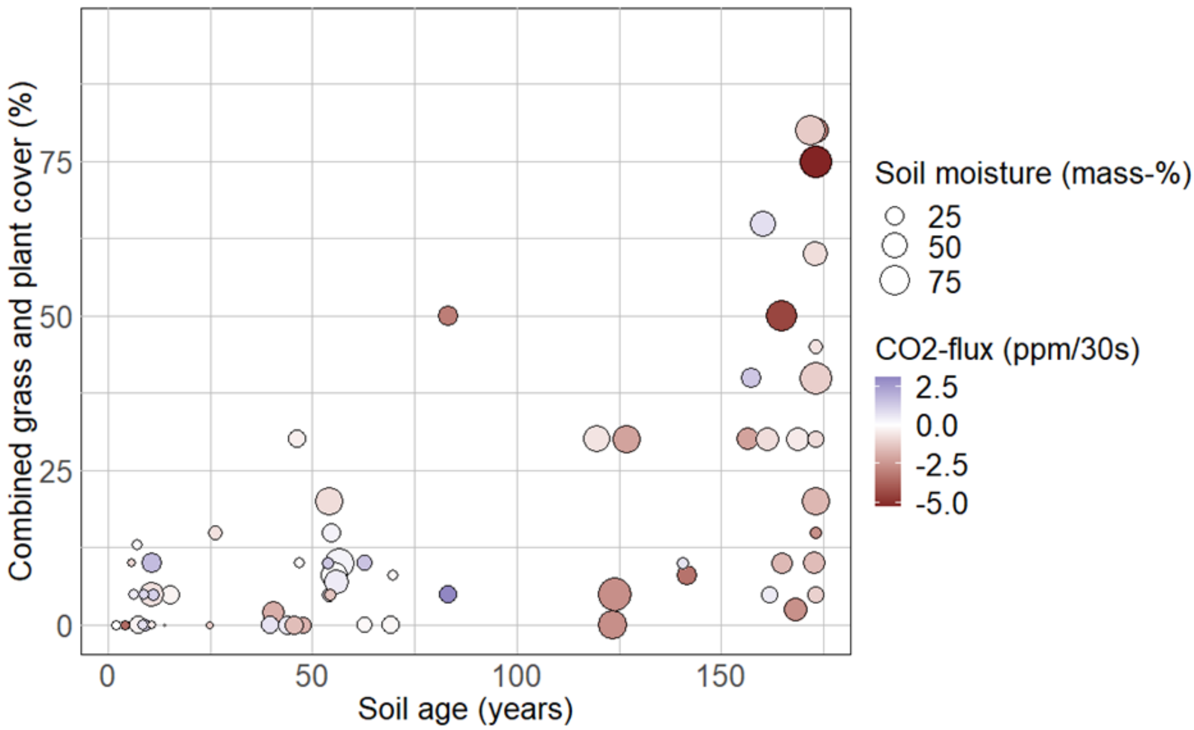

Figure 14: Scatter plot with soil age on the x-axis and total vegetation cover percentage excluding moss on the y-axis. The colour of the dots depicts the CO_2-fluxes, with positive fluxes in blue, and negative fluxes in brown-red. Larger dots represent higher soil moisture mass-percentages.

Table 1: Means and standard errors of different variables based on soil age categories. Soil moisture, pH and OM are all measured in the upper soil horizon.

Parameter	Ages 0-40 (n=25)	Ages 40-84 (n=23)	Ages 119-174 (n=29)
Flux (ppm / 30s)	-0.00219 ± 0.258	0.00226 ± 0.282	-1.46 ± 0.289
Soil moisture mass-%	14.5 ± 2.16	26.7 ± 3.62	44.9 ± 4.42
pH	5.27	4.77	4.47
Elevation (m)	2734 ± 15.0	2684 ± 8.76	2506 ± 12.4
OM mass-%	2.44 ± 0.781	9.02 ± 2.42	23.9 ± 4.27
Moss-%	13.6 ± 4.40	33.1 ± 5.63	23.6 ± 4.36
Grass-%	2.52 ± 0.863	4.32 ± 1.07	22.9 ± 4.06
Plant-%	1.43 ± 0.444	5.23 ± 2.08	7.68 ± 2.72

ditions of low soil moisture. This observation suggests the involvement of one or more additional processes that significantly contribute to the observed flux dynamics.

Table 1 depicts mean and standard error values for the different variables for the time periods 0 to 40 years, 40 to 84 years and 119 to 174 years. These periods correspond to the colour schemes in Figure 13. What is remarkable, is that both from ages 0 to 40 and 40 to 84 the mean flux is effectively zero. This is despite the fact between these two categories there has been a large increase in soil moisture, OM mass-percentage and total vegetation-percentage. In the first two categories, moss is the only vegetation type that averages a presence of more than 10 percent of the surface cover. In the oldest category, the presence of grass was greatly increased, whereas moss decreased relative to the category of ages 40 to 84. Plant are not found in great quantities throughout the whole field site. Furthermore, there is a steady decrease of pH, indicating a gradual acidification of the soil, all the way into the ages 119 to 174 category. In this last category a clear negative mean CO_2-flux (-1.46) is found. Additionally, the highest soil moisture, OM and total vegetation are found in this category.

Multiple linear regression of the variables soil age, soil moisture, total vegetation and pH suggests that only soil moisture is significant in such a model ($p = 0.03$). Soil age ($p = 0.34$), total vegetation ($p = 0.64$) and pH ($p = 0.27$) are not. The model itself is significant, with a p-value of 0.001. The adjusted R^2 is 0.20, meaning that this model explains 20% of the variation in the CO_2-flux. Variance inflation factors of these variables range from 1.38 to 1.68, which is comfortably lower than 5, indicating low multicollinearity. Therefore, multicollinearity is not a problematic issue in this analysis.

3.4 Organic matter

From the regression between the mass-percentage of organic matter found in soils and the CO_2-fluxes at these locations a negative correlation is visible (Figure 15). It is generally accepted to convert organic matter to organic carbon by multiplying by the Van Bemmelen conversion factor of 0.58 (Heaton et al., 2016), but since this would highly amplify the uncertainty of the data the choice was made to use the measured organic matter values for this analysis. The mass-percentage of organic matter is not normally distributed, the flux-data is. The Spearman's rank correlation coefficient is -0.41 ($p = 2.5 \times 10^{-4}$). This is a moderate negative correlation. While this is a clear pattern, it is not enough to confidently use CO_2-fluxes as an approximation for the total organic matter stored in the concerning soils. Additionally, Figure 15 shows that the highest organic matter percentages were generally found at locations where grass is the dominant vegetation type.

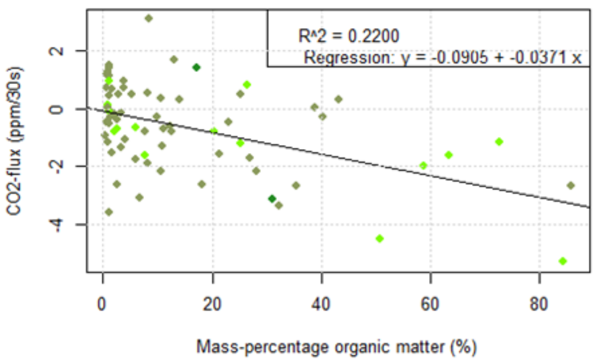

Figure 15: Regression of organic matter mass-percentage against CO_2-fluxes. The colour scheme corresponds to the dominant vegetation colours, with moss in moss-green, grass in bright green and plants in dark-green.

3.5 Further results

The regression between the measured soil moisture and the Topographic Wetness Index that was used as a proxy for soil moisture to determine the soil sampling locations does not suggest any correlation (Figure 16). Apparently, the TWI was not a suitable method to use as an approximation for the soil moisture. Nonetheless, there is still a good distribution of soil moisture values.

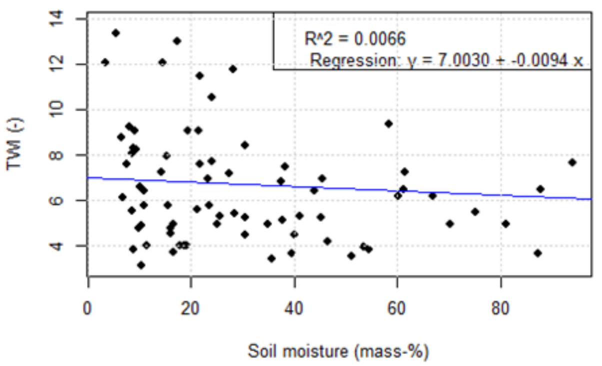

Figure 16: Regression of measured soil moisture mass-percentages against Topographic Wetness Index values.

The PCA (Figure 17) confirms the impressions from the previous results, namely that soil moisture, soil age, total vegetation and organic matter are all negatively related to the CO_2-fluxes. All of these parameters are strongly tied to dimension one, which explains 38% of the total variance. Together with principal component two, over 50% of the total variance is explained. Grass cover has the same type of negative relation, whereas plant cover is slightly less related in the first dimension. Moss is mostly related to the second dimension of variance. The value of pH is strongly tied to the measured CO_2-fluxes.

Whether precipitation has an influence on the flux was also researched. Since most of the investigated variables do have a clear pattern from younger to older soils, it is necessary to investigate the possible influence of precipitation on CO_2-fluxes in a region where there is a good distribution of different precipitation circumstances. This is only the case on the lower plateau (circled in red in Figure 18), because this plateau was visited on most days during the field campaign. Therefore, this analysis was conducted with only locations inside the circle. What becomes clear from Figure 19 is that on dry measurements (over 12 hours without precipitation), CO_2-fluxes average above zero, with a median of 0.775 ppm/30s. In all of the other precipitation conditions, fluxes average a negative value, becoming increasingly negative with time since last precipitation. During rainy conditions (R), the median is -1.598. Up to one hour after rain (R1), it is -1.742. From 1 to 12 hours after a precipitation event (R12), it is -2.168. These sets of data are all normally distributed. The ANOVA results in a p-value of 0.11, indicating that

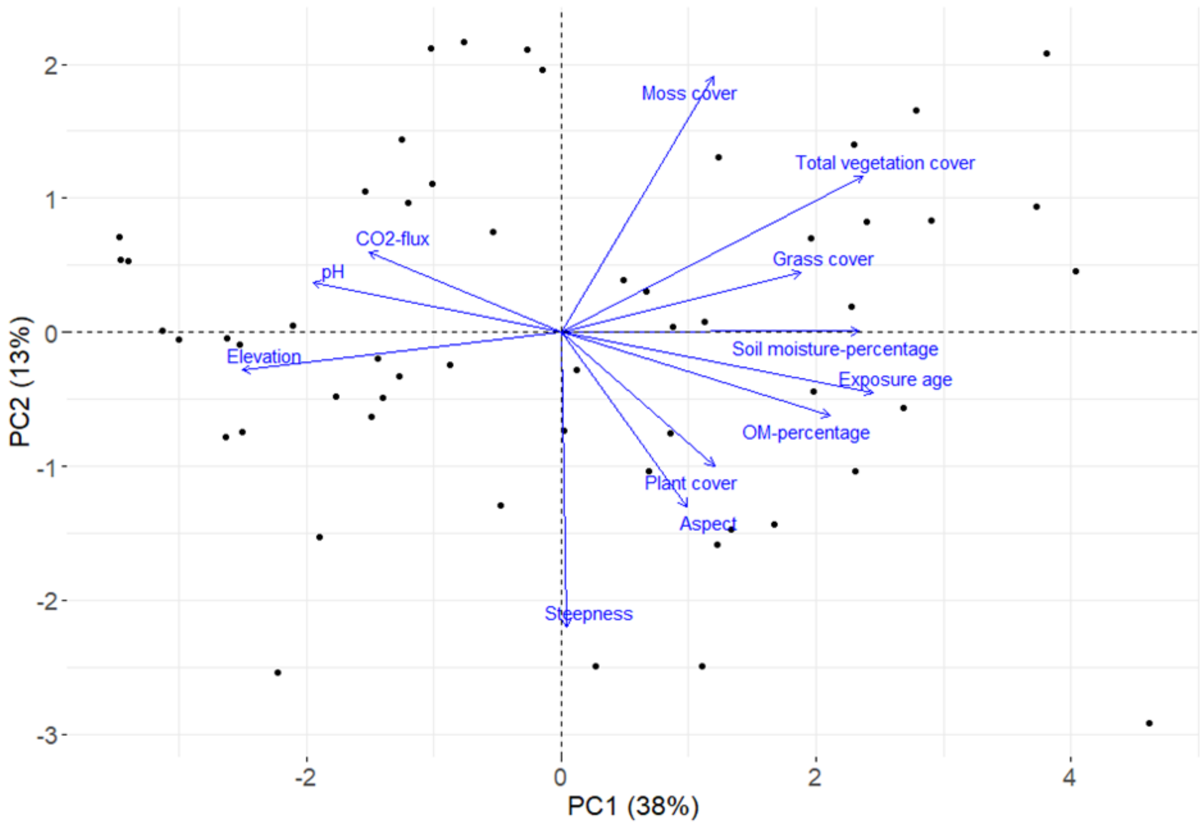

Figure 17: Principal component analysis of different numerical variables, based on the 55 locations that have information on all of the selected variables.

there is no evidence for a significant CO_2-flux difference caused by precipitation conditions.

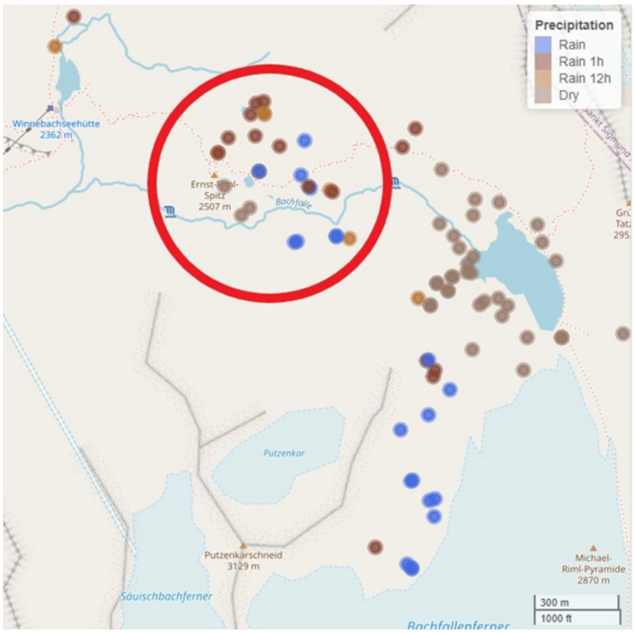

Figure 18: Encircled in red the location of the "lower plateau", where measurements were conducted in a mix of different precipitation conditions. Meaning of the different categories: Dry = over 12 hours without rain at the moment of measurement. Rain 12h = less than 12 hours since last rain. Rain 1h = less than 1 hours since last rain. Rain = rain during measurement.

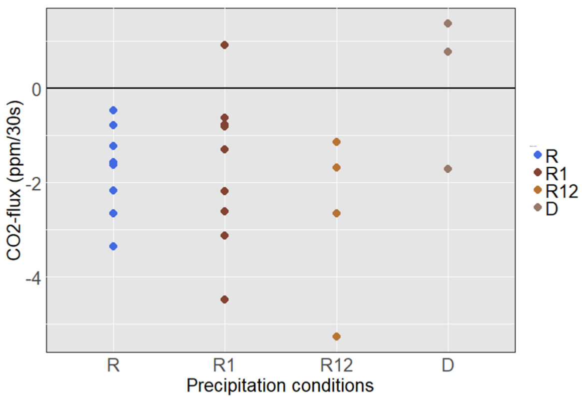

Figure 19: Dotted plot of precipitation circumstances on the lower plateau. D = dry (n = 3), R = precipitation (n = 8), R1 = precipitation in the last hour (n = 10), R12 = precipitation in the last 12 hours (n = 4).

The mass-percentage of soil moisture is highly correlated with the mass-percentage of organic matter in dry soil. Both variables are not normally distributed. The spearman's rank correlation coefficient is 0.91, which indicates a very high correlation.

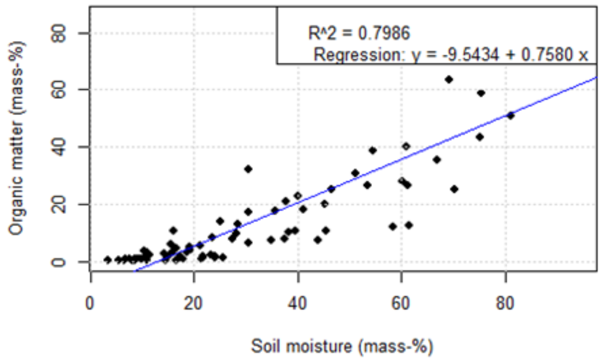

Figure 20: Regression of soil moisture mass percentages against organic matter mass-percentages.

4 Discussion

4.1 Assessment of methodology

Limitations of Topographic Wetness Index (TWI)

The regression between the Topographic Wetness Index and the actual measured soil moisture suggests that there is hardly any relation between the two ($R^2 = 0.066$), indicating that in this case the TWI was not a suitable proxy for the soil moisture as input for the Latin hypercube sampling method. This could be partly due to weather conditions, since there were multiple days of precipitation before and during the field campaign. Additionally, the TWI is a one-dimensional method. It is only based on elevation differences. Kopecký and Čížková (2010) point out that TWI relies on a number of theoretical assumptions, including uniform soil properties. This limitation seems to hurt the accuracy of TWI in the heterogeneous Bachfallenferner region. Especially the capacity of soils to retain water seemed to play a large role in the actual soil moisture distribution during the field campaign. Consequently, measured soil moistures mainly show which soils have this capacity. This ability is greater in fine, vegetated, OM-rich soils, and less so in bare, coarse soils. Furthermore, the soils in the area are predominantly shallow and located on poorly permeable parent material. In these soils micro-topography becomes relatively more important compared to the landscape position which is used by the TWI. The 10×10m grid used as input for the TWI is not fine enough to register this variation. Nevertheless, there is still a decent distribution of soil moisture values, so the inaccuracy of TWI did not have an adverse effect on the research.

Averaging flux measurements per location

Four flux measurements were conducted per location (two spatial and two temporal replicates). Flux coefficients were based on averaging all approved flux measurements ($R^2 \geq 0.7$) per locations. Consequently, not all locations were averaged over all four fluxes (Table 2). For locations where multiple measurements were approved, the mean difference between lowest and highest measured flux on a single location was 2.95 ppm/30s. For only locations where all four flux measurements were approved, the range between lowest and highest flux averages 3.77 ppm/30s. The lowest flux (-5.27, location W15) and the highest flux (3.06, location Y18) used in the analyses differ by merely 8.33 ppm/30s. This is a rather large range, indicating a large measurement uncertainty. In the data that used all four fluxes, no evidence was found for a bias in the data (e.g. spatial replicates consistently forming two groups, which could indicate observable differences between spatial replicate sites inside one location). Causes of the variability of measurements include noise by air passing through an imperfectly fitted chamber. Furthermore, the linear regression method used to derive the flux at each location takes at least 5 data points, for a total of 2 minutes. This could result in an underestimation of the initial flux. Kutzbach et al. (2007) showed that nonlinear exponential regression models were frequently more suitable than linear regression models for determining initial fluxes with a closed-chamber method, even with short measurement times. Especially higher absolute flux coefficients are at risk of being underestimated, in extreme cases linear regression models were found to register fluxes as low as 40% of the ones found with nonlinear exponential regression models (Kutzbach et al., 2007). Averaging the fluxes increased the validity of the values used in the analysis, and the trends found in the results support this. Therefore, the gathered data are considered to be adequate in describing relations between the flux and the various other variables. The higher absolute flux-values are likely to be underestimated to some extent. For an accurate estimation of the error, the data could be re-analysed in the future, using a nonlinear exponential regression model.

Table 2: Ranges between highest and lowest measured flux, grouped based on the amount of fluxes used to calculate the coefficient of each location.

Group	n	Mean range	Median range
1 flux	14	0.00	0.00
2 fluxes	25	2.00	1.36
3 fluxes	19	3.24	2.83
4 fluxes	22	3.77	2.95
2+3+4 fluxes	66	2.95	2.43

Assessment of surface cover types

Abundance of moss, grass, plants, bare rock, stones, fine earth and surface water was determined by personal judgement. Although the majority of these variables are easily distinguishable, assigning them all a percentage of surface cover unavoidably comes with an error of judgement. Besides, grass and plants are slightly more difficult to interpret and therefore more prone to being assigned the wrong category. Morrison (2016) found that the mean coefficient of variance was often 25 to 50 percent between different observers of common species. This was due to a combination of the characteristics of vegetation itself and attributes of the observer. As the field campaign group did not consist of plant ecology experts, at least similar variance can be expected.

Lab data

Soil moisture and organic matter values used for the analyses were exclusively taken from the upper horizon of every measurement location. In most cases this was either an Ah horizon or a C horizon. Further topsoil horizon types were H, Cg and Cr. Mean depths of Ah and H horizons were 4.49 cm, whereas this value was 12.31 cm for C, Cg and Cr horizons. Since organic matter (and by extent soil moisture) generally decreases with depth, soil moisture contents of deeper soils could be slightly underestimated. For the full dataset there is a slight correlation ($R^2 = 0.06$) between top horizon depth and soil moisture, which could to some extent be influenced by this. This correlation is not found in a dataset using only topsoils shallower than 13 cm, even though this dataset still consists for 25% out of C-horizons (including Cg and Cr). Using only topsoils shallower than 13 cm, soil moisture explains 18.0% of the variation in CO_2-fluxes, as opposed to 21.4% in the full dataset. Refer to Appendix C for figures.

Furthermore, the used soil samples were stored in sealed plastic bags for several days, and were transported in heavy bags which might have influenced measurements. Especially samples that contained high amounts of soil moisture may have had moisture leaching out following the impact of gravity and pressure applied heavy materials on top of them. At the start of lab analysis, some of the bags had a small pool of water in them. Therefore, soil moisture contents of especially wet soils could be slightly underestimated.

4.2 Role of soil moisture and vegetation in proglacial soil development

The results indicate that wetlands do not significantly differ from their relatively dry soil counterparts in terms of CO_2-fluxes. However, that does not discount the influence that soil moisture has on CO_2-fluxes. Soil moisture is identified as a primary variable of influence concerning CO_2-uptake. This includes but is not limited to wetlands. Other soils with a high soil moisture content could be hotspots for CO_2-uptake as well. It should however be noted that these results are influenced by the fact that no measurements have been conducted after an extended period of drought, soils were likely more saturated than on an average summer day. In non-proglacial soils, CO_2-effluxes can be reduced by reduced gas diffusivity and air-filled porosity caused by heavy rainfall (B. C. Ball., 1999). A period of drought may have provided different results for the comparison between wetlands and other soils, and for measured CO_2-fluxes in general. The amount of data in relation to rainfall was not of sufficient size to provide significant results.

Research on Svalbard by Szymański et al. (2019) confirms that out of parent material, vegetation cover and site wetness, the latter is most influential regarding the variability of soil properties. However, it surprisingly finds that wet soils did not contain more organic carbon than dry soils, but moist soils did. These results differ from the ones found in this paper, which found that the most organic matter was present in the wettest soils. With a Spearman's rank correlation of 0.91 the direct influence that these variables have on each other is evident. This is unsurprising, seeing that organic matter can significantly affect soil moisture holding (Lal, 2020). However, locations with high soil moisture are not only found due to higher organic matter content, usually it is the other way around. Often, geophysical factors such as topography cause certain locations to be more beneficial than others regarding soil moisture accumulation. Out of the 23 wetlands visited during the field campaign, 13 were located in a local depression. From the remaining 68 visited soils, only 2 were located inside a depression. Lower lying areas where moisture accumulates seem to be primary locations for soils development in proglacial area. Soil moisture appears to be a crucial factor in the weathering process in these areas (Egli et al., 2006). Additionally, it has an essential role, alongside grain size of parent material, in the establishment of plants in a primary succession on nutrient-poor sites (Burga, 1999). Early development of primary succession can accelerate the succession into higher order vegetation.

Furthermore, high soil moisture levels are important in inhibiting respiration (Han et al., 2018). Koch et al. (2008) found that in fens and wet fens, respiration was negatively correlated to water-filled pore space. This is caused by anoxic conditions created by high soil moisture levels, while aerobic respiration is the main source of CO_2 emissions. Also, water-logging may prevent CO_2-diffusion in the soil matrix, resulting in lower soil CO_2 emissions (Koch et al., 2008).

Conversely, this does not apply to the meadow and dry fen locations in the Koch et al. (2008) research, which indicates that these soil types have a respiration rate positively correlated to water-filled pore space, as these soils were very low in soil moisture and thus water limited. Water stress causes a reduction of gross primary production through photosynthesis as well, further limiting CO_2-uptake by vegetation (Green et al., 2019).

Vegetation was determined to be significant influential factor regarding CO_2-fluxes in the area. Since moss is known to be of low photosynthetic activity (Aro and Gerbaud, 1984), mainly grasses and plants are expected to have a role in the uptake of CO_2. The regression analyses suggest grasses are the most important vegetation type in the research area, but this has not been confirmed by the ANOVA. Nonetheless, while moss is identified as a dominant vegetation species throughout the field site, an increase of CO_2-uptake is observed only along the latter stages of the chronosequence. Grass and plants were observed to a greater extent in older soils at lower elevations. Generally, grasslands become more common during the intermediate successional stage with soil ages from 40 to 80 years (Eichel, 2019). In the research area indeed a slight increase of grasslands is observed during this period, but these species become dominant only from soil age 119 onwards.

According to Eckmeier et al. (2013), after 50 years, soils tend to get more suitable for plant growth, and switch their main source of carbon from ancient to modern. To see the effect this has on fluxes, an additional one-sided t-test was done. Both soils older and younger than 50 years were normally distributed. The p-value from the t-test is 0.03, indicating that older soils do indeed take up more CO_2 than younger soils, but this result is not as highly significant as the result from the t-test between soils younger than 84 and older than 119 years. This indicates that it is likely that while soils might be more suitable for plant growth after 50 years, the effects of this on the flux coefficient become more pronounced only after a few more decades.

4.3 Additional factors and future research

The variables covered in the results are not sufficient to present a full overview of the factors influencing CO_2-fluxes, as is evident from the results section in which the variables are combined. There are further relevant variables that have not been extensively discussed yet. One of these is microbial activity, of which the abundance in the area of research is unknown, but is it safe to assume that these communities increase in biomass and diversity with soil age and soil development (Esperschütz et al., 2011). In the previous subsection it has been established that high soil moisture levels inhibit respiration through the creation of anoxic conditions. Furthermore, soil acidification could have a role in reducing activity of microbes, thereby reducing respiration rates (Reth et al., 2005). In non-proglacial grasslands, Čuhel et al. (2010) observed significantly higher CO_2-emissions by microbial communities around neutral pH conditions (pH of 6.82 $\pm$ 0.40) as compared to acidic soil conditions (pH of 5.52 $\pm$ 0.48). The pH conditions found in the field site range from 5.27 in the youngest soil category to 4.47 in the oldest soil category, indicating that pH may have had an influence on CO_2-emissions. Another limiting factor for microbial activity could be a lack of available C. Older soils have been observed to possess greater amounts of physically and chemically recalcitrant organic matter, as opposed to labile organic matter which can be used by microbial communities. At the Damma glacier in Switzerland this has resulted in a C-limited inhibition of bacterial growth (Göransson et al., 2011). This recalcitrant C appears to be a primary source of energy in both very newly exposed soils (before there is any significant labile C-source, (Bardgett et al., 2007)), and in older soils where labile C has already been used up (Hahn and Quideau, 2013; Bradley et al., 2014).

Soil temperatures were not measured during the field campaign, but have been shown to have a large and exponential influence on respiration rates in the Eastern Austrian Alps, especially during nighttime (Koch et al., 2008). Higher soil temperatures are more commonly present in areas of lower elevation, and may therefore reduce negativity of the fluxes found in the older soils. Fang and Moncrieff (2001) showed that soil respiration was positively related to temperature up to at least 32 degrees Celsius, although in extremer cases it could induce water stress and thereby have an adverse effect on respiration rates (Oertel et al., 2016). Fluxes found in the research area were more consistently negative compared to other carbon flux experiments conducted in the Alps (Koch et al., 2008; Rogiers et al., 2005). The unusually low summertime temperatures during the field campaign (often between 0 and 5 degrees Celsius during daytime), may have had a role in decreasing respiration and thereby lowering CO_2-fluxes. Research at the Schrankogel (less than 10 km from the Bachfallenferner proglacial area) found increased microbial biomass at lower elevations (2700 to 2900 m compared to 3000 to 3100 m and 3200 m+), with especially archaeal abundance found to be significantly correlated only to soil temperature (Hofmann et al., 2016). For further research it could be relevant to include soil temperature measurements.

It is worth mentioning that flux measurements were done in August, which does not adequately represent the yearly cycle that is characterized by seasonal variability of photosynthetic and respiratory activity. Furthermore, the measurements were only conducted during daytime, and therefore are not representative values for daily averages. Both photosynthesis and respiration follow a diurnal cycle, with photosynthesis being an active process only during daytime and respiration increasing during nighttime. Koch et al. (2008) found that nighttime respiration values peaked in August in both its study years (2003 and 2004). This could be related to the higher soil temperatures during this time of year. The dryer the soil type, the more respiration was found. Remarkably, the main conclusion of Koch et al. (2008) is completely opposite of what is found in this research: wet fens (corresponding to wetlands in this paper) registered the lowest daytime CO_2-influx by a considerable margin.

Cumulative daytime CO_2-fluxes in the snow-free period of 149 days in 2003, expressed in (g C $\times$ m$^{-2}\times$ period^{-1}), ranged from 218 in meadows to 84 in wet fens. Converting the mean CO_2-flux values found in wetlands of the Bachfallenferner glacier (-1.48 ppm/30s), results in a mean daytime C accumulation of 464g C $\times$ m$^{-2}\times$ period^{-1}. Results for the older soils in general are approximately the same (-1.46 ppm/30s, accumulation of 458g C$\times$ m$^{-2}\times$ period^{-1}). Daily daytime values (assuming a daytime of 14 hours and 45 minutes) for these older soils are 1.89g C$\times$ m$^{-2}\times$ d^{-1} or 6.92g $CO_2\times$ m$^{-2}\times$ d^{-1}. These values are remarkably high, likely due to the fact that all measurements were conducted during August, which is the peak accumulation period in the Koch et al. (2008) study as well. Daytime values for only August were not retrievable from that study. This pattern is consistent with flux measurements conducted in a reed wetland in northern China, which found peak daily CO_2-uptake in July (-13.58 g $CO_2\times$ m$^{-2}\times$ d^{-1}), reducing to fluxes around 0 in October (Zhou et al., 2009). This underlines the need for a multi-seasonal field campaign for any study with the goal is to accurately represent annual C-accumulation. Furthermore, nighttime measurements are crucial to quantify C-losses through soil respiration.

In order to correct for weather differences, a "radiation filter" was used as described in the methods. Three variables were used to compare the influence of the filter on the R^2. In all three of the cases, the difference was less than 0.02. For soil moisture mass-% (Figure 21, Table 3), R^2 improved from 0.2198 to 0.2237. Soil age and organic matter mass-% give a similar picture. In every case, the maximum addition factor was positive for sunny condi-

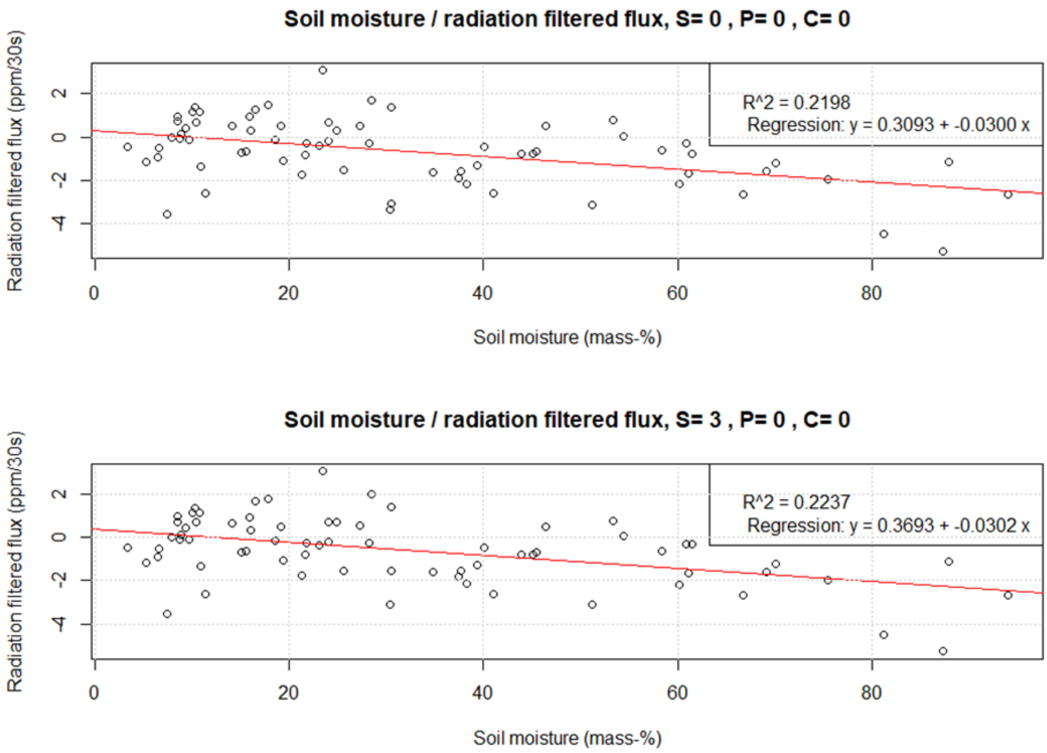

Figure 21: Regressions of soil moisture mass-percentages against CO_2-fluxes. The top figure has no radiation filter applied. The bottom figure has the radiation filter with maximum additions that reach an optimal R^2. S = Sunny, P = Partly cloudy, C = Cloudy.

Table 3: R^2 of regression of different variables with and without radiation filter. The max additions represent the optimal addition values per cloud condition for an R^2 as high as possible.

Variable	**Normal regression R^2**	**Filtered regression R^2**	**Max additions**		
			Sunny	**Partly cloudy**	**Cloudy**
Soil moisture	0.2198	0.2237	3.0	0.0	0.0
Soil age	0.1752	0.1875	6.0	0.0	0.0
Organic matter	0.2303	0.2490	5.7	3.3	0.0

tions, and 0 in cloudy conditions. This consistent pattern does suggest that sunny conditions (and therefore radiation) do at least somewhat increase photosynthesis. In other words, a better fit is reached when compensating for the effect of radiation on photosynthesis. Nonetheless, the effect of radiation does not greatly influence the relations found between the different variables. General conclusions on relations between these variables can be made, even without taking into account differences in radiation. In partly cloudy situations the correction is maximum 3.3 for total organic matter, while there is none for the soil moisture and soil age regressions.

Although there was a large difference between the measured fluxes in dry conditions and the (recent) precipitation conditions on the lower plateau, it is worth mentioning that the amount of data points used was small. For respectively R (rain during measurement), R1 (less than one hours since rain), R12 (less than 12 hours since rain) and D (dry; over 12 hours without rain), $n = 3$, $n = 8$, $n = 10$ and $n = 4$. This is a large reason for the insignificance of these results

In a further study it could be relevant to have a flux chamber dedicated to one location, on which fluxes are measured throughout the day (and if possible, night) and subject to different intensities of light, radiation, temperatures and precipitation. This would allow for a more robust estimation of the influence of these environmental variables.

4.4 Impact of future climate change

The Alps are expected to endure accelerated warming throughout the 21st century, with increased intensities of temperature and precipitation extremes and more severe drought regimes (Gobiet et al., 2014). This will significantly impact the future carbon cycle of proglacial areas. First of all, increased soil temperatures are likely to increase soil respiration rates exponentially (Koch et al., 2008). Furthermore, increased occurrance of weather extremes may lead to more drought and moisture-limited conditions in the area. Drying of wetlands is associated with increased carbon emissions, especially through the loss of CH_4. Globally, wetland CH_4-emissions are even the largest natural source of the methane budget, contributing roughly one third to total natural and anthropogenic emissions (Zhang et al., 2017). Since soil moisture is a significant influential factor the accumulation of organic carbon in proglacial areas, it is safe to assume increased emissions from these areas as well during periods of drought. Soils with normally high soil moisture content will more often revert from anoxic to oxic conditions, increasing respiration rates. Additionally, the period of snow cover during winters will most likely decrease, which will increase the time period in which CO_2-exchange is an active process. This could either increase or decrease the potential carbon budget of proglacial soils, depending on whether the sign of the mean CO_2-flux is positive or negative in these new circumstances.

5 Conclusion

Soil moisture is shown to be a primary variable of influence regarding CO_2-fluxes of proglacial soils. While no significant distinction could be observed between wetlands and their dry soil counterparts, soil moisture values display a moderate negative correlation with the flux coefficient. A likely influential process involved is reduction of microbial respiration due to anoxic conditions. Locations with a high soil moisture content were often found in local depressions, indicating that these types of sites could be locations with a large potential to accumulate carbon. Soil moisture was found to correlate very strongly with the presence of organic matter. Organic matter, and by extent organic carbon, is moderately correlated to the flux coefficient as well, but not sufficiently for the flux coefficient to be suitable as a proxy for carbon accumulation in proglacial soils. From the different types of vegetation, grass was most strongly correlated to the flux coefficient, whereas moss was only weakly correlated. An insufficient amount of locations with plants as dominant vegetation was present to yield any conclusion on this vegetation type. In the chronosequence, a remarkable difference was found between soils younger than 84 years and older than 119 years. In the younger age categories mean daytime flux coefficients are all around zero, whereas the older age category displays a clear negative mean flux of -1.46 ppm/30s. This cannot only be explained by the influence of soil moisture and vegetation, since older soils show a negative flux even if these values are low. An influential factor in this may be the lower pH in older soils, because it can limit CO_2-emissions compared to neutral pH. Radiation does appear to have some influence on the measured daytime fluxes, but variables related to the flux can be sufficiently distinguished without taking this factor into account. Precipitation could not be significantly related to the measured fluxes, partly due to a lack of representative data.

Climate change is likely to enhance proglacial carbon emissions through increased respiration due to higher soil temperatures and increased emissions due to more frequent drought events. To get a complete view of the role of proglacial areas in the carbon budget more research is needed. This should include soil temperature as a variable. Furthermore, it would be relevant to conduct a multiple-day measurement on a single location throughout the diurnal cycle, which could grant valuable insight into the influence of various environmental variables such as temperature, precipitation and radiation. Lastly, more inter-seasonal measurements are needed to determine annual flux rates.

Acknowledgements

I would like to thank my supervisors Sigrid van Grinsven and Ryan Teuling for their support and insights given during this thesis. Their feedback and guidance were of great help throughout the past half year. Furthermore, I would like to thank Arnaud Temme for his help with ArcGIS-modelling in preparation of the field campaign. I want to thank Collin van Rooij, Laura Wildschut, Tomba Paagman and again Sigrid van Grinsven and Arnaud Temme for the fun and productive field campaign. It was a real team effort to gather this much data in less than a week time. On that note, the warm reception and care given by the personnel of the Winnebachseehütte was of great aid as well. Lastly, I want to thank the HWM thesis-ring for their often very helpful feedback, which guided me into the right direction numerous times.

References

Alagna, K. E., Peccerillo, A., Martin, S., and Donati, C. (2010). Tertiary to Present Evolution of Orogenic Magmatism in Italy. *Journal of the Virtual Explorer*, 36(June 2014).

ArcGIS Pro (2023). ArcGIS Pro.

Aro, E.-m. and Gerbaud, A. (1984). co 2 c 3. III:867–870.

B. C. Ball., A. Scott., J. P. P. (1999). Adsorption Kinetics of CO 2 , O 2 , N 2 , and CH 4 in Cation-Exchanged Clinoptilolite. *Soil and Tillage Research*, 53:1313–1319.

Bardgett, R. D., Richter, A., Bol, R., Garnett, M. H., Bäumler, R., Xu, X., Lopez-Capel, E., Manning, D. A., Hobbs, P. J., Hartley, I. R., and Wanek, W. (2007). Heterotrophic microbial communities use ancient carbon following glacial retreat. *Biology Letters*, 3(5):487–490.

Bastviken, D. (2015). Supplement of Technical Note: Cost-efficient approaches to measure carbon dioxide (CO 2) fluxes and concentrations in terrestrial and aquatic environments using mini loggers The copyright of individual parts of the supplement might differ from the CC-BY . 12:3849–3859.

Bradley, J. A., Singarayer, J. S., and Anesio, A. M. (2014). Microbial community dynamics in the forefield of glaciers. *Proceedings of the Royal Society B: Biological Sciences*, 281(1795).

Burga, C. A. (1999). Vegetation development on the glacier forefield Morteratsch (Switzerland). *Applied Vegetation Science*, 2(1):17–24.

Čuhel, J., Šimek, M., Laughlin, R. J., Bru, D., Chèneby, D., Watson, C. J., and Philippot, L. (2010). Insights into the effect of soil pH on N2O and N2 emissions and denitrifier community size and activity. *Applied and Environmental Microbiology*, 76(6):1870–1878.

data.gv (2023). Digitales Geländemodell (DGM) Österreich.

Eckmeier, E., Mavris, C., Krebs, R., Pichler, B., and Eg, M. (2013). Black carbon contributes to organic matter in young soils in the Morteratsch proglacial area (Switzerland). *Biogeosciences*, 10(3):1265–1274.

Egli, M., Wernli, M., Kneisel, C., and Haeberli, W. (2006). Melting glaciers and soil development in the proglacial area Morteratsch (Swiss Alps): I. Soil type chronosequence. *Arctic, Antarctic, and Alpine Research*, 38(4):499–509.

Eichel, J. (2019). *Geomorphology of Proglacial Systems*.

Eralp, A. E. and Tomson, M. B. (1978). pH Averaging pH = pKa + logic joL ? (3). 50(2):389–392.

Esperschütz, J., Pérez-De-Mora, A., Schreiner, K., Welzl, G., Buegger, F., Zeyer, J., Hagedorn, F., Munch, J. C., and Schloter, M. (2011). Microbial food web dynamics along a soil chronosequence of a glacier forefield. *Biogeosciences*, 8(11):3283–3294.

Fang, C. and Moncrieff, J. B. (2001). The dependence of soil CO2 efflux on temperature. *Soil Biology and Biochemistry*, 33(2):155–165.

FreeWorldMaps (2023). Austria Map.

Gobiet, A., Kotlarski, S., Beniston, M., Heinrich, G., Rajczak, J., and Stoffel, M. (2014). 21st century climate change in the European Alps-A review. *Science of the Total Environment*, 493:1138–1151.

Göransson, H., Olde Venterink, H., and Bååth, E. (2011). Soil bacterial growth and nutrient limitation along a chronosequence from a glacier forefield. *Soil Biology and Biochemistry*, 43(6):1333–1340.

Green, J. K., Seneviratne, S. I., Berg, A. M., Findell, K. L., Hagemann, S., Lawrence, D. M., and Gentine, P. (2019). Large influence of soil moisture on long-term terrestrial carbon uptake. *Nature*, 565(7740):476–479.

Guelland, K., Hagedorn, F., Smittenberg, R. H., Göransson, H., Bernasconi, S. M., Hajdas, I., and Kretzschmar, R. (2013). Evolution of carbon fluxes during initial soil formation along the forefield of Damma glacier, Switzerland. *Biogeochemistry*, 113(1-3):545–561.

Hahn, A. S. and Quideau, S. A. (2013). Shifts in soil microbial community biomass and resource utilization along a Canadian glacier chronosequence. *Canadian Journal of Soil Science*, 93(3):305–318.

Han, G., Sun, B., Chu, X., Xing, Q., Song, W., and Xia, J. (2018). Precipitation events reduce soil respiration in a coastal wetland based on four-year continuous field measurements. *Agricultural and Forest Meteorology*, 256-257(January):292–303.

Heaton, L., Fullen, M. A., and Bhattacharyya, R. (2016). Critical Analysis of the van Bemmelen Conversion Factor used to Convert Soil Organic Matter Data to Soil Organic Carbon Data: Comparative Analyses in a UK Loamy Sand Soil. *Espaço Aberto*, 6(1):35–44.

Hofmann, K., Lamprecht, A., Pauli, H., and Illmer, P. (2016). Distribution of Prokaryotic Abundance and Microbial Nutrient Cycling Across a High-Alpine Altitudinal Gradient in the Austrian Central Alps is Affected by Vegetation, Temperature, and Soil Nutrients. *Microbial Ecology*, 72(3):704–716.

Janssen, E. M. (2023). CO 2 fluxes of a glacier forefield. (January):1–39.

Koch, O., Tscherko, D., Küppers, M., and Kandeler, E. (2008). Interannual ecosystem CO2 dynamics in the alpine zone of the eastern alps, Austria. *Arctic, Antarctic, and Alpine Research*, 40(3):487–496.

Kopecký, M. and Čížková, (2010). Using topographic wetness index in vegetation ecology: Does the algorithm matter? *Applied Vegetation Science*, 13(4):450–459.

Kotlarski, S., Bosshard, T., Lüthi, D., Pall, P., and Schär, C. (2012). Elevation gradients of European climate change in the regional climate model COSMO-CLM. *Climatic Change*, 112(2):189–215.

Kutzbach, L., Schneider, J., Sachs, T., Giebels, M., Nykänen, H., Shurpali, N. J., Martikainen, P. J., Alm, J., and Wilmking, M. (2007). CO2 flux determination by closed-chamber methods can be seriously biased by inappropriate application of linear regression. *Biogeosciences*, 4(6):1005–1025.

Lal, R. (2020). Soil organic matter and water retention. *Agronomy Journal*, 112(5):3265–3277.

Maplogs, S. (2023). Sunrise maplogs Winnebachseehütte.

Mavris, C., Egli, M., Plötze, M., Blum, J. D., Mirabella, A., Giaccai, D., and Haeberli, W. (2010). Initial stages of weathering and soil formation in the Morteratsch proglacial area (Upper Engadine, Switzerland). *Geoderma*, 155(3-4):359–371.

Minasny, B. and McBratney, A. B. (2006). A conditioned Latin hypercube method for sampling in the presence of ancillary information. *Computers and Geosciences*, 32(9):1378–1388.

Mitsch, W. J., Bernal, B., Nahlik, A. M., Mander, , Zhang, L., Anderson, C. J., Jørgensen, S. E., and Brix, H. (2013). Wetlands, carbon, and climate change. *Landscape Ecology*, 28(4):583–597.

Moomaw, W. R., Chmura, G. L., Davies, G. T., Finlayson, C. M., Middleton, B. A., Natali, S. M., Perry, J. E., Roulet, N., and Sutton-Grier, A. E. (2018). Wetlands In a Changing Climate: Science, Policy and Management. *Wetlands*, 38(2):183–205.

Morrison, L. W. (2016). Observer error in vegetation surveys: A review. *Journal of Plant Ecology*, 9(4):367–379.

Noll, M. and Wellinger, M. (2008). Changes of the soil ecosystem along a receding glacier: Testing the correlation between environmental factors and bacterial community structure. *Soil Biology and Biochemistry*, 40(10):2611–2619.

NSIDC (2023). Global Land Ice Measurements from Space (GLIMS).

Oertel, C., Matschullat, J., Zurba, K., Zimmermann, F., and Erasmi, S. (2016). Greenhouse gas emissions from soils—A review. *Chemie der Erde*, 76(3):327–352.

Painter, T. H., Flanner, M. G., Kaser, G., Marzeion, B., Van Curen, R. A., and Abdalati, W. (2013). End of the Little Ice Age in the Alps forced by industrial black carbon. *Proceedings of the National Academy of Sciences of the United States of America*, 110(38):15216–15221.

Pro, G. E. (2023). Google Earth Pro.

Reth, S., Reichstein, M., and Falge, E. (2005). The effect of soil water content, soil temperature, soil pH-value and the root mass on soil CO2 efflux - A modified model. *Plant and Soil*, 268(1):21–33.

Rogiers, N., Eugster, W., Furger, M., and Siegwolf, R. (2005). Effect of land management on ecosystem carbon fluxes at a subalpine grassland site in the Swiss Alps. *Theoretical and Applied Climatology*, 80(2-4):187–203.

Roulet, N. T. (2000). Peatlands, carbon storage, greenhouse gases, and the kyoto protocol: Prospects and significance for Canada. *Wetlands*, 20(4):605–615.

Salimi, S., Almuktar, S. A., and Scholz, M. (2021). Impact of climate change on wetland ecosystems: A critical review of experimental wetlands. *Journal of Environmental Management*, 286(January):112160.

Schlesinger, W. H. (1990). Evidence from chronosequence studies for a low carbon-storage potential of soils. *Nature*, 348(6298):232–234.

SenseAir (2023). SenseAir K33 ELG.

Sinclair, T. R. and Horie, T. (1989). Leaf nitrogen, photosynthesis, and crop radiation use efficiency: A review. *Crop Science*, 29(1):90–98.

Smittenberg, R. H., Gierga, M., Göransson, H., Christl, I., Farinotti, D., and Bernasconi, S. M. (2012). Climate-sensitive ecosystem carbon dynamics along the soil chronosequence of the Damma glacier forefield, Switzerland. *Global Change Biology*, 18(6):1941–1955.

Sommer, C., Malz, P., Seehaus, T. C., Lippl, S., Zemp, M., and Braun, M. H. (2020). Rapid glacier retreat and downwasting throughout the European Alps in the early 21st century. *Nature Communications*, 11(1).

Sørensen, R., Zinko, U., and Seibert, J. (2006). On the calculation of the topographic wetness index: Evaluation of different methods based on field observations. *Hydrology and Earth System Sciences*, 10(1):101–112.

Szymański, W., Maciejowski, W., Ostafin, K., Ziaja, W., and Sobucki, M. (2019). Impact of parent material, vegetation cover, and site wetness on variability of soil properties in proglacial areas of small glaciers along the northeastern coast of Sørkappland (SE Spitsbergen). *Catena*, 183(October 2018):104209.

Zemp, M. (2006). Glaciers and Climate Change Spatio-temporal Analysis of Glacier Fluctuations in the European Alps after 1850. *Analysis*, page 67.

Zemp, M., Paul, F., Hoelzle, M., and Haeberli, W. (2008). Glacier Fluctuations in the European Alps, 1850-2000. In Orlove, B., Wiegandt, E., and Luckman, B. H., editors, *Darkening Peaks: Glacier Retreat, Science, and Society*, pages 152–167. University of California Press.

Zhang, Z., Zimmermann, N. E., Stenke, A., Li, X., Hodson, E. L., Zhu, G., Huang, C., and Poulter, B. (2017). Emerging role of wetland methane emissions in driving 21st century climate change. *Proceedings of the National Academy of Sciences of the United States of America*, 114(36):9647–9652.

Zhou, L., Zhou, G., and Jia, Q. (2009). Annual cycle of CO2 exchange over a reed (Phragmites australis) wetland in Northeast China. *Aquatic Botany*, 91(2):91–98.

A Sampling sheets

The sheets used during the field campaign.

Location description Bachfallenferner fieldwork summer 2023

General:
- Start new location on a new page in field-notebook
- Sampling locations have leading zeroes: S01, S02, W01, etc, up to 10.
- Additional locations (not of pre-selected sampling list) get an ID between 900 and 1000 (example: S905).
- Picture naming is done manually in the evening or afterwards. Naming follows format: S35_A (for 10m2 picture)
- No empty cells: if no answer, then write NA

To be recorded:
Location ID
Type of location (Soil/Wetland/Lake)
Date of observation (YY/M/D)
Time of observation (24h notation, HH:MM)
Group (A,B,C)

Action: take pictures
A: $10m^2$ incl backpack
B: 1 m^2 surface location
C: Chambers + outside iButton
D: As above, but with chambers removed.

Questions:
Weather
Wt1. It is sunny (S); partly cloudy (P); cloudy/overcast (C)
Wt2. It is raining (R); has rained or snowed in the last hour (R1); has rained or snowed in the last 12H (R12); dry (D).

Location (10m distance /100m2 area based)
Lo1. GPS coordinates as measured at location.
Lo2. Steepness measured over 10m dist (degrees).
Lo3. Slope orientation/aspect (degrees out of 360, with 0=360=north-facing).
Lo4. Plan curvature (concave, straight, convex, complex)
Lo5. Profile curvature (concave, straight, convex, complex)
Lo5b. If complex, zoom in and repeat L3 and L4. If not, write NA.
Lo6. Signs of erosion or deposition? (ero/dep/no)
Lo7. Currently or in the past connected to a river system? (current/past/no).
Lo8. Should this location be considered a wetland? (yes/no/maybe)
Lo9. Should this location be considered a local depression (yes/no/maybe)

Surface (all from 1m2)

Fill in table with % of m2 cover:

Bare hardrock	
Stone	
Fine earth	
Grass	
Plant	
Moss	
Surface water	
Total %	*

* if not 100%, add explanation at comments

Su1. Largest size of stones (cm)
Su2. How much of the 100 m2 plot is the same as your selected 1 m2 plot? More than 50% or less than 50%? If less than 50%, note in the comments what is the other surface cover, and why you selected this location instead.
Su3. Additional comments, anything special.

Soil sampling

H1. Wetness of soil at 10 cm depth (saturated/moist/dry)

Per horizon:

H2: Horizon ID. Example: S43_Ah
H3: Horizon code (Ol, Ah, Bw, C, Cg, Cr etc)
H4. Horizon start depth (cm)
H5. Horizon end depth (cm)
H6. Texture (after removal of gravel and larger, use triangle p27). Record the abbreviation (S / LS/SL/SCL etc)
H7. Total rock fragments in horizon (percentage of the soil volume)
H8. Rock fragment size (dominant size, but see p46).
H9. Rock fragment shape (flat, angular, subrounded, rounded)
H10. Soil structure grade (no, weak, moderate, strong, see table)
H11. Soil structure type (Single Grain, GRanular, SubAngular blocky, see table + image)
H12. Root abundance (estimate number of roots per dm^2 /100 cm^2, even if your horizon is thinner than 10cm)
H13. Root size (average, in mm).
H14. Describe any bio activity in horizon other than roots. If nothing; NA
H15. Additional comments regarding the horizon, anything not covered above. If nothing; NA

Action:
Take a sample of the fine earth fraction of the horizon, aiming for 50 to 100g of fine earth. Rocks can be in the sample, but should not count towards the 50-100 g. Add pencil-written piece of paper to sample bag with horizon ID, and also write horizon IDon sample bag with sharpie. Horizon ID is e.g. S43_Ah.

Flux sampling

Flux measurement

Of each individual measurement (**4x**):

F1: Measurement ID (LocationID_number of spatial replicate_number of sampling moment)
Example: S35_R1_M1
F2: Chamber ID
F3: Date (YY/MM/DD)
F4: Time at placement of chamber (time in 24h notation, HH:MM:SS)
F5: Ttime at removal of chamber (time in 24h notation, HH:MM:SS)
F6: iButton ID inside
F7: iButton ID outside
F8: Flux measurement comments?

Per sampling location (**1x**):

F9: LocationID (Example: S35)
F10a: For spatial replicate R1: Expected quality of box-soil connection: (Good/Medium/Bad)
F10b: For spatial replicate R2: Expected quality of box-soil connection: (Good/Medium/Bad)
F11: Air flow through soil expected? (Y/N)
F12: Is chamber location between your two spatial replicates the same? (Y/N). If N, comment.
F13: Are the chamber locations representative for the 10x10m surroundings? If N, comment.
F14: Comments about flux sampling location?

B Shapiro-Wilk test results

Type	Nr	Shapiro-Wilk
Wetlands – coupled soils		
Wetlands	14	0.70
Soils	14	0.61
Soil moisture – Fluxes		
Soil moisture	77	7.1*10^-6
Fluxes	77	0.055
Moisture classes		
Low	51	0.08
Middle	21	0.91
High	8	0.58
Soil Moisture – Fluxes in soils > 119y		
Soil moisture	32	0.17
Fluxes	32	0.64
Vegetation cover – Flux		
Total vegetation	74	6.6*10^-4
Moss	74	1.3*10^-6
Grass	74	1.3*10^-11
Plants	74	1.7*10^-14
Fluxes	74	0.14
Vegetation higher 50 lower 30		
Flux higher 50	33	0.69
Flux lower 30	32	0.13
Soil age flux regression		
Soil age	77	7.2*10^-8
Fluxes	77	0.22
Fluxes younger older 50		
Younger 50	77	0.43
Older 50	77	0.88
Fluxes younger older 80		
Younger 80	77	0.33
Older 80	77	0.64
Organic matter – flux		
Organic matter	77	7.8*10^-11
Fluxes	77	0.55
Soil moisture – organic matter		
Soil moisture	77	7.1*10^-6
Organic matter	77	7.8*10^-11
Fluxes precipitation conditions		
D	3	0.35
R	8	0.91
R1	10	0.93
R12	4	0.40

C Soil horizon depth

Additional data on soil horizon depth, and its correlation with soil moisture.

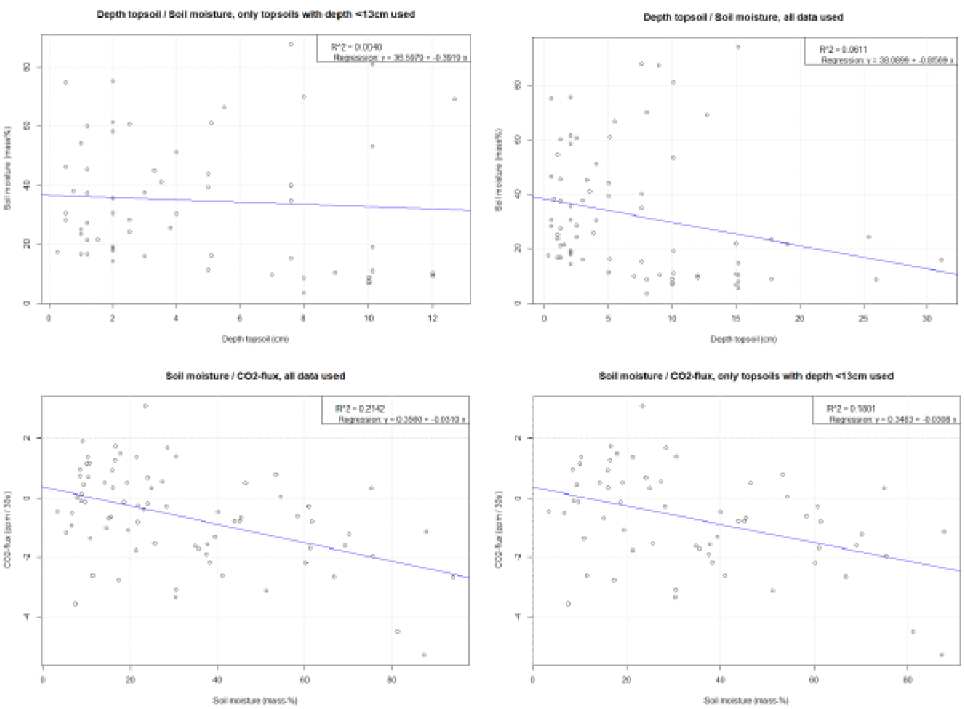

Topsoil type	Nr	Mean (cm)	Median (cm)
Ah, H	51	4.49	2.5
C, Cg, Cr	28	12.31	12